Faculdade de Engenharia da Universidade do Porto

Power electronics based modernization of electrical power infrastructure in railway systems

Francisco Roleira de Carvalho

Master in Electrical and Computer Engineering

Supervisor: António José de Pina Marins

June 30, 2023

Abstract

Railways have been a part of human history for a long time, as a means of transportation for both people and goods. The means used to supply locomotives with the power required to move have evolved through time, and electric power is gaining an increasingly higher influence in this area, with the growing number of electrified railways around the world.

The process of supplying locomotives with power in electrified railways reliably and efficiently comes with many problems and challenges, mostly regarding the need to respect different standards. To mitigate or eliminate some of these problems, various methods have been the subject of studies and tests. Some of them have been applied throughout the history of electrified railways. This dissertation briefly describes how the energy gets from the utility source to the railway lines giving a historical perspective on the evolution of the supplying conditions. It also provides an overview of some of the main standards to be met, with a greater focus on the ones currently in use in the European Union, and the main groups of solutions currently in use for this energy-supplying process. The groups of solutions mentioned are the use of substations based on transformers and the use of substations based on power electronics converters or both. The solutions involving power electronics are given bigger emphasis as these are still relatively new, and not widely spread. Their characteristics are better suited for achieving the main goals of an efficient power supply to the railway system, and therefore their simulation and understanding are of greater importance for this work and the future of this area.

Preliminary studies were conducted to understand how the locomotive's relative position and power factor impact the catenary´s voltage values and the power flow from the substations to the locomotive. The main component of this work consists of the design of a model of a power electronics-based substation, with an AC/DC conversion module based on an NPC converter capable of extracting power from a regular three-phase AC transmission/distribution grid and transforming it into DC power (Vdc=42 kV), and a DC/AC conversion module based on an MMC structure that transforms that DC power into single-phase AC power (Vac=27.5 kV, 50 Hz) that can be supplied to a catenary. These modules are the subject of different simulations that look to replicate real railway situations with some realism and show both their strengths and limitations. As a final design and simulation component, a controlled model of two substations working in parallel was developed and tested under

different scenarios, to study how the developed substation modules can cope with the target of feeding multiple locomotives, in different locations and with different power demands and power factors, including some that are regenerating power.

Keywords – Conversion module, locomotive, power electronics, railway, substation

Resumo

O transporte ferroviário faz parte da história da humanidade há muito tempo, como meio locomoção tanto para pessoas como para mercadorias. Os meios utilizados para fornecer às locomotivas a energia necessária para se deslocarem têm evoluído ao longo do tempo, e a energia elétrica está a ganhar uma influência cada vez maior nesta área, com o crescente número de linhas eletrificadas em todo o mundo.

O processo de fornecimento de energia às locomotivas em linhas eletrificadas de forma fiável e eficiente traz consigo muitos problemas e desafios, principalmente no que diz respeito à necessidade de respeitar diferentes normas. Para mitigar ou eliminar alguns destes problemas, vários métodos têm sido objeto de estudos e testes. Alguns deles têm sido aplicados ao longo da história das ferrovias eletrificadas. Esta dissertação descreve brevemente como a energia chega da fonte até às linhas ferroviárias, dando uma perspetiva histórica sobre a evolução das condições de fornecimento. Também fornece uma visão geral de algumas das principais normas a cumprir, com um maior enfoque nas atualmente em uso na União Europeia e nos principais grupos de soluções atualmente em uso para este processo de fornecimento de energia. Os grupos de soluções mencionados são o uso de subestações baseadas em transformadores e o uso de subestações baseadas em conversores eletrónicos de potência ou ambos. As soluções que envolvem eletrónica de potência são enfatizadas pois são ainda relativamente novas e não amplamente difundidas. As suas características são mais adequadas para alcançar os principais objetivos de um fornecimento de energia eficiente ao sistema ferroviário e por isso a sua simulação e compreensão são de maior importância para este trabalho e para o futuro desta área.

Foram realizados estudos preliminares para compreender como a posição relativa e o fator de potência da locomotiva afetam os valores de tensão da catenária e o fluxo de energia das subestações para a locomotiva. A principal componente deste trabalho consiste no projeto de um modelo de uma subestação baseada em eletrónica de potência, com um módulo de conversão AC/DC baseado num conversor NPC capaz de extrair energia de uma rede AC trifásica normal de transporte ou distribuição e transformá-la em energia DC (Vdc=42 kV) e um módulo de conversão DC/AC baseado numa estrutura MMC que transforma essa energia DC em energia

AC monofásica (Vac=27.5 kV, 50 Hz) que pode ser entregue a uma catenária. Estes módulos são objeto de diferentes simulações que procuram replicar situações reais de linhas ferroviárias com algum realismo e mostrar tanto as suas vantagens como as suas limitações. Como componente final de projeto e simulação, foi desenvolvido e testado um modelo controlado de duas subestações a trabalhar em paralelo, sob diferentes cenários, para estudar como os módulos de subestação desenvolvidos podem lidar com o objetivo de alimentar várias locomotivas, em diferentes locais e com diferentes exigências e fatores de potência, incluindo algumas que estão a regenerar energia.

Agradecimentos

Gostaria de começar por agradecer ao professor António Pina Martins por se ter mostrado sempre disponível e empenhado em me acompanhar e orientar ao longo do desenvolvimento do meu trabalho de dissertação.

Também quero agradecer aos meus amigos, desde a infância até agora, por serem uma parte muito significativa da minha vida e da pessoa que sou hoje.

Por último, quero agradecer à minha família, e em particular aos meus pais, por me terem sempre apoiado ao longo do meu percurso pessoal e académico.

Index

Abstract iii

Resumo v

Agradecimentos vii

Index ix

List of figures xi

List of tables xiii

Abbreviations and Symbols xv

Chapter 1 1

Introduction 1
- 1.1 - Motivation 1
- 1.2 - Structure 2
- 1.3 - Methodology and tools 2

Chapter 2 5

Background, fundamental aspects, and electrification solutions 5
- 2.1 - Historical context 5
- 2.2 - Supplying electrified railways with power 6
- 2.3 - Main requirements and standards 7
- 2.4 - Electrification involving transformers 10
- 2.5 - Electrification involving power electronics 10
- 2.6 - Conclusions 16

Chapter 3 17

Load models and static characteristics 17
- 3.1 - Locomotive models in simulations 17
- 3.2 - First study 18
- 3.3 - Second study 20
- 3.4 - Third study 21
- 3.5 - Fourth study 22
- 3.6 - Conclusions 23

Chapter 4 25

Design and test of a railway substation 25
- 4.1 - Design of the three-phase AC/DC conversion module 25
- 4.2 - Testing of the three-phase AC/DC conversion module 29
- 4.3 - Testing of the single-phase DC/AC conversion module 35

4.4 - Testing of the single-phase DC/AC conversion module 37
4.5 - Conclusions 45

Chapter 5 47

Control and simulation of two substations in parallel 47
5.1 - Development of a control system for the overall model 48
5.2 - Simulation of the two substations in parallel mode 50
5.3 - Conclusions 60

Chapter 6 61

Conclusions and future work 61
6.1 - Conclusions 62
6.2 - Future work 63

References 53

List of figures

Figure 2.1- Power conversion in an electrified railway, modified from [2]. 6
Figure 2.2 - Substation based on a transformer, [3]. 6
Figure 2.3 - Representation of a 2x25 kV feeding system, [2]. 7
Figure 2.4 - Schematic use of an SVC in railways, [12]. 11
Figure 2.5 - Substation with STATCOM technology, [13]. 11
Figure 2.6 - Back-to-back converter, adapted from [1]. 12
Figure 2.7 - Single-phase cascaded H-bridge with multiple dc-links, adapted from [1]. 13
Figure 2.8 - Direct AC/AC MMC, [14]. 14
Figure 2.9 - Indirect AC/AC MMC, modified from [15]. 14
Figure 2.10 - Cophase system, [16]. 15
Figure 2.11 – Advanced cophase system, [17]. 15
Figure 3.1 - Representation of a locomotive through an impedance. 17
Figure 3.2 - Representation of a locomotive through a current source. 18
Figure 3.3 - Representation of a locomotive through a PQ load. 18
Figure 3.4 - Representation of the conditions in which the first and second studies were conducted. 19
Figure 3.5 - Voltage variation with the distance between the locomotive and the substation. 19
Figure 3.6 - Voltage variation with the power factor of the locomotive. 20
Figure 3.7 - Representation of the conditions in which the third and fourth studies were conducted. 21
Figure 3.8 - Voltage variation with the distance between the locomotive and the first substation. 22
Figure 3.9 - Apparent power consumption varies with the distance between the locomotive and the first substation. 23
Figure 4.1 - AC/DC NPC converter. 26
Figure 4.2 - Obtention of theta. 27
Figure 4.3 - ABC-dq0 transformation. 27
Figure 4.4 – Idref and Iqref generation for unitary power factor. 27
Figure 4.5 - Control signals generation 28
Figure 4.6 - Modulation 28
Figure 4.7 - Grid connecting side voltage values. 30
Figure 4.8 - Simple and line-line voltage values at the converter. 30
Figure 4.9 - Current in phase A in the first test. 30
Figure 4.10 - DC link voltage in the first test. 31
Figure 4.11 - Power supplied in the first test. 31
Figure 4.12 - DC link voltage in the second test. 32
Figure 4.13 - Currents on the three-phase side in the second test. 33
Figure 4.14 - Power supplied in the second test. 33
Figure 4.15 - DC link voltage in the third test. 34
Figure 4.16 - Power supplied in the third test. 34
Figure 4.17 - Currents on the three-phase side in the third test. 35
Figure 4.18 - Submodules of two transistors (half-bridge) with a capacitor in parallel. 36
Figure 4.19 - Connection between both ends of each arm and LC filter. 36
Figure 4.20 - Generation of the control signal. 37
Figure 4.21 - Generation of final control signals. 37
Figure 4.22 - Output voltage in the first simulation. 38
Figure 4.23 - Voltage in the upper left arm in the first simulation. 38

Figure 4.24 - Output voltage (RMS) in the first simulation. 39
Figure 4.25 - Output current in the first simulation. 39
Figure 4.26 - Voltage in two capacitors in different arms. 40
Figure 4.27 - Voltage in the transistor. 40
Figure 4.28 - Carrier waves. 40
Figure 4.29 - Output voltage (RMS) in the second simulation. 41
Figure 4.30 - Current in the catenary in the second simulation. 41
Figure 4.31 - Output voltage in the transitory period of the second simulation. 42
Figure 4.32 - Current in the DC end of the second simulation. 42
Figure 4.33 - Output voltage (RMS) in the third simulation. 43
Figure 4.34 - Current in the catenary in the second simulation. 44
Figure 4.35 - Current in the DC end of the third simulation. 44
Figure 4.36 – Output voltage in the fourth simulation. 45
Figure 4.37 – Output current in the fourth simulation. 45
Figure 5.1 - Average model of a substation. 47
Figure 5.2 - Potential positions of the locomotives in the simulations. 48
Figure 5.3 - Control circuit of the first substation. 49
Figure 5.4 - Generation of the delta value for the second substation´s voltage phase angle. 50
Figure 5.5 - Generation of the signal responsible for controlling the phase angle of the second substation´s voltage phase angle. 50
Figure 5.6 - Control circuit of the second substation. 50
Figure 5.7 - Relative position of the locomotives in the first scenario. 51
Figure 5.8 - Working timeline of Locomotive 1 in the first scenario. 51
Figure 5.9 - Working timeline of Locomotive 2 in the first scenario. 52
Figure 5.10 - Working timeline of Locomotive 3 in the first scenario. 52
Figure 5.11 - Working timeline of Locomotive 4 in the first scenario. 52
Figure 5.12 - Total power injected into the catenary by each substation in the first simulation of the first scenario. 53
Figure 5.13 - Total power injected into the catenary by each substation in the second simulation of the first scenario. 54
Figure 5.14 - Relative position of the locomotives in the second scenario. 56
Figure 5.15 - Working timeline of Locomotive 1 in the second scenario. 56
Figure 5.16 - Working timeline of Locomotive 2 in the second scenario. 56
Figure 5.17 - Working timeline of Locomotive 3 in the second scenario. 56
Figure 5.18 - Working timeline of Locomotive 4 in the second scenario. 56
Figure 5.19 - Total power injected into the catenary by each substation in the first simulation of the second scenario. 57
Figure 5.20 - Total power injected into the catenary by each substation in the second simulation of the second scenario. 59

List of tables

Table 2.1 - Supply voltage limits (root mean square (RMS) values), [5]. 8
Table 2.2 - Voltage harmonic planning levels according to IEC 61000-3-6, [8][9]. 9
Table 2.3 - Total inductive power factor (λ) of a train, modified from [10]. 9
Table 5.1 - Power losses in the first simulation of the first scenario 53
Table 5.2 - Voltage in Position 3 in the second simulation of the first scenario. 54
Table 5.3 - Power losses in the second simulation of the first scenario. 55
Table 5.4 - Voltage in Position 3 in the second simulation of the first scenario. 55
Table 5.5 - Power losses in the first simulation of the second scenario. 57
Table 5.6 - Voltage in Position 3 in the first simulation of the second scenario. 58
Table 5.7 - Power losses in the second simulation of the second scenario. 59
Table 5.8 - Voltage in Position 3 in the second simulation of the second scenario. 59

Abbreviations and Symbols

List of abbreviations

AC	Alternating Current
DC	Direct Current
EHV	Extra-High-Voltage
HMT	High-Voltage Matching Transformer
HS	High-Speed
HV	High-Voltage
Hz	Hertz
IEC	International Electrotechnical Commission
km	Kilometer
MMC	Modular Multilevel Converter
MV	Medium-Voltage
NPC	Neutral Point Clamped
PI	Proportional-Integral
PLL	Phase-Locked Loop
PWM	Pulse Width Modulation
RMS	Root Mean Square
SM	Submodule
SVC	Static VAR Compensator
SVM	Space Vector Modulation
Sub.	Substation
TEN	Trans-European Rail Network
TCR	Thyristor Controlled Reactor
TEN	Traction Matching Transformer
THD	Total Harmonic Distortion
TSC	Thyristor Switched Capacitor
TSI	Technical Specifications for Interoperability
TT	Traction Transformer
VOC	Voltage Oriented Control

List of symbols

A	Ampere
C	Capacitor
F	Farad
H	Henry
L	Inductance
P	Active power
S	Apparent power
V	Volt
W_P	Active energy
W_Q	Reactive energy
Z	Impedance
δ	Phase difference
λ	Power factor
Ω	Ohm
ω	Frequency

Chapter 1

Introduction

This chapter looks to expose the motivations behind this dissertation work, by giving an initial overview of the subject, and the reasons why it was picked. It also provides a brief description of the structure of the document, the methodology, and the tools used.

1.1 – Motivation

In our world, railways are extremely important for the economy, as the fastest means of land transportation for both people and goods. Currently, most railways are nonelectrified, with the trains being diesel-powered. This comes with some challenges and problems associated. The diesel-powered trains require the existence of multiple refueling stations, because they are not in permanent contact with their energy supplier, unlike electricity-powered ones. Plus, diesel-powered trains result in high levels of noise and air pollution. The air pollution, in particular, is a big issue given the growing concerns of humanity with emissions and global warming and the increasing number of programs and plans to make the economy more environmentally friendly. However, some railways are electrified, and the trains are supplied directly by the pantographs. These are in contact with a catenary that delivers power that was taken and converted by a substation from a source, usually the power grid. Thanks to this way of supplying the locomotives with energy, these tend to be both more powerful and lighter. On the other hand, constructing an electrified railway is significatively more expensive on initial capital and maintenance costs. As a result, it is only justified in cases where lines have high levels of traffic, [1].

There are lots of challenges associated with designing an efficient electrified railway. Some of the main difficulties in supplying an electrified railway system include the reduction of power losses, the avoidance of voltage drops associated with high levels of traffic on the line (high loads), the reduction of the imbalance impact on the utility grid due to AC traction loads

(trains) and the effective conversion of three-phase power into single-phase power. Consequently, the main goal when projecting the supply system of these railways is trying to mitigate or even eliminate these issues, considering the traffic on the line, and the costs involved in building, operating, and maintaining the network, [1].

Although there are already many solutions in place, the permanently growing global economy has led to an increase in the number of people and goods to be transported and the consequent construction of new high-speed lines around the world, especially in China, the United States, and Europe. This combined with the increasingly stricter regulations imposed by utility grid owners when it comes to the introduction of imbalances is changing the way people look at the more conventional options. As a result, there is a progressively bigger push to study, develop and optimize new ways of achieving the mentioned goals, which has led to great developments. Nevertheless, this is still an understudied area as there is still a lot to explore to optimize and modernize the energy infrastructure of the railway systems, [1].

Considering the different areas that an electrical engineering student is exposed to, electronics and problem-solving to achieve goals considering efficiency, cost, and the health of the environment have been two of the most captivating ones for me, and picking a dissertation project that combined these was one of my targets. Among the different dissertation themes available for choice, this one managed to combine both in an interesting way and allowed me to explore an area that I find interesting but knew very little about. This led to this choice for the dissertation project.

1.2 – Methodology and tools

Regarding the methodology, it consisted first in collecting information about the topic, namely about the different standards and solutions available. After that, it consisted in designing power electronics systems, namely a three-phase AC/DC converter and a single-phase DC/AC converter, and simulating them to make sure the project met the required goals. It also consisted in designing and simulating a model of two substations working in parallel.

Multiple software was considered to pick the ones that satisfy the needs of the different components of this project. When it comes to time domain simulations both PSIM´s and MATLAB Simulink´s characteristics were analyzed, and both have most of the tools required, namely the ability to build and simulate power electronics models. Ultimately, PSIM was picked as the software to be used, because of its easier understanding interface. For scripts and graphics development, MATLAB was the picked software. It was mostly used in the preliminary studies.

1.3 – Structure

This document is divided into 6 chapters.

Chapter 1 provides an initial overview of the topic and the motivations behind its choice. It also provides a description of the methodology and tools used and the structure.

Chapter 2 gives a more detailed analysis of the theme and its implications. This includes a historical perspective, the main standards to be respected, and the different solutions currently in use.

Chapter 3 presents different ways of representing a locomotive in a simulation and a few preliminary studies regarding voltage drop in the catenary and power flow.

Chapter 4 describes the power electronics behind the project of a substation model, namely the converter´s characteristics, with a particular focus on the control component. It also shows and discusses the most important results taken from the simulation of the converter and discusses its positives and negatives.

Chapter 5 describes how two substations can be controlled to work in parallel, and presents different results taken from simulating this situation under different scenarios.

Chapter 6 presents the main conclusions and provides a proposal for future work.

Chapter 2

Background, fundamental aspects, and electrification solutions

This chapter provides an overview of the main aspects of the electrified railway. It presents a historical context and discusses the main solutions and International and European standards to be met.

2.1 – Historical context

The first step towards the electrification of the railways came with the electrification of the tramway, making trams the first rail-based transportation means to be powered by electricity. This electrification consisted of a direct current, low-voltage supply, typically below 750 V. After that, came the first electrified mainlines, using a three-phase alternating current supply. This montage was characterized by two overhead wires and a third wire which was the running rails and had very demanding requirements for the pantograph system, [1].

It was only after the end of World War I that the electrified railway systems started getting closer to the ones that are currently common. In this period, countries like Austria, Germany, Norway, Sweden, and Switzerland started adopting a single-phase alternating-current system, with a voltage of 15 kV and a frequency of 16.67 Hz. At the same time, some other European countries kept direct-current networks, operating at voltages of 1 kV and 3 kV, [1].

The further development of high-power converters led to independence between the supply type and the traction system. Consequently, single-phase alternating-current systems with a nominal voltage of 25 kV and frequency of 50 Hz became the most popular solution, spreading all over the world. Thanks to the 50 Hz frequency, which is the same as the power grid in most of the world, except America and some parts of Asia, feeder stations became simpler and transmission losses were reduced, [1].

2.2 – Supplying electrified railways with power

To get the trains moving, electrified railway infrastructures must get energy from a source, most of the time the utility grid, convert it, and transfer it to the catenary responsible for supplying the locomotives. This happens thanks to substations/feeder stations strategically spread across the lines, connecting the energy source to the railway system, as shown in the Figure 2.1 diagram. Each substation is represented by Sub., [2].

In a more specific analysis, each substation has the main goal of converting the three-phase power from the utility grid into single-phase power that can be used to supply the trains. As a secondary goal, it can also convert the single-phase power resulting from trains that may be regenerating due to braking into three-phase power that can be injected back into the utility grid. Figure 2.2 presents a diagram of a single substation, based on a transformer. In both Figures 2.1 and 2.2, the substations are connected to pairs of successive phases, on the catenary end, [3].

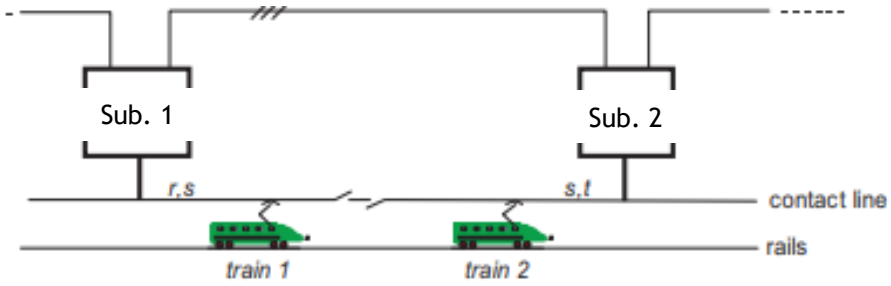

Figure 2.1- Power conversion in an electrified railway, modified from [2].

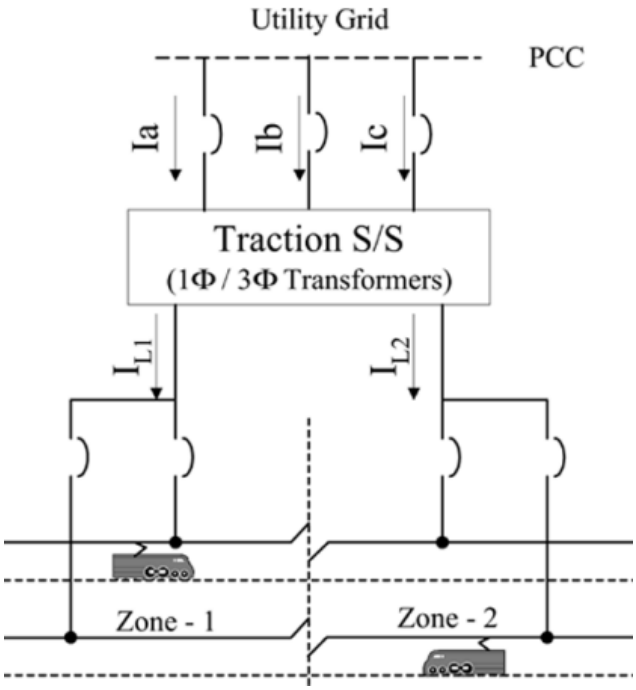

Figure 2.2 - Substation based on a transformer, [3].

While the overall process of supplying the locomotives can be relatively simple, doing so in a good way is extremely challenging. It is necessary to respect different standards established by organizations such as the International Electrotechnical Commission (IEC). In European Union countries it is also necessary to respect European standards, which are mostly in accordance with IEC standards. Therefore, the big challenge of this area is studying different solutions and equipment that can be used in the design of the substations, taking into consideration the standards mentioned, the traffic level on the railway, and the characteristics of the locomotives that will circulate there. It is important to achieve the goals mentioned before in a cost-efficient manner.

Besides the most widespread system, which is the 1x25 kV one, a relatively new architecture called 2x25 kV is growing fast and is currently used for some high-speed lines in France, Italy, Japan, and Spain, among others. Its characteristics include transmitting power at 50 kV, thanks to a feeder at -25 kV, creating a total voltage difference between the feeder and the contact wire messenger of 50 kV. This higher voltage value results in power transmission with lower currents and, consequently, reduces losses. It also results in reduced voltage drops. These are useful characteristics in high-speed lines, where the power values are higher. In Figure 2.3 there is a representation of a 2x25 kV feeding system, [2].

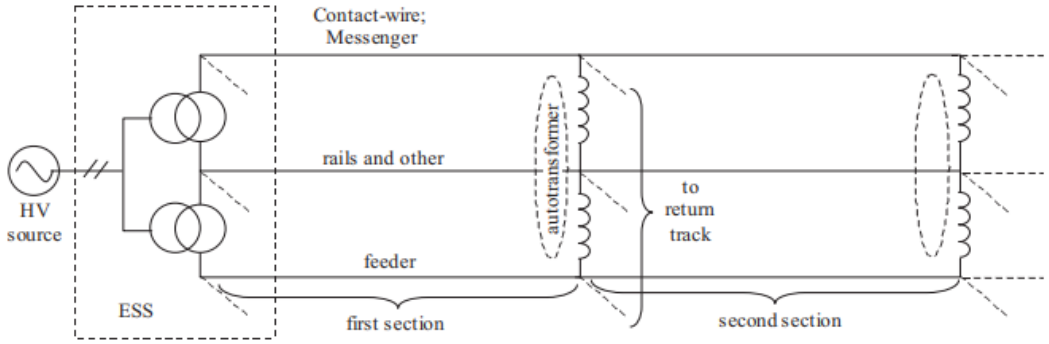

Figure 2.3 - Representation of a 2x25 kV feeding system, [2].

2.3 – Main requirements and standards

The power supplied to the railway systems in European Union countries must respect the parameters established in EN 50160, a European Standard that must be respected by all European Union countries in their national standards, [4].

When it comes to the supply voltage, its nominal frequency must be 50 Hz. As for potential deviations, the mean value of the fundamental frequency measured over a period of 10 seconds must always be kept between the nominal value minus 6% and the nominal value plus 4%. This implies that this measurement must stay between 47 Hz and 52 Hz. It must also stay within a plus/minus 1% range 99.5% of the time, each year, meaning that it can only fall

below 49,5% or exceed 50,5% during 0,5% of the year. These rules apply to systems with a synchronous connection to an interconnected system [4].

For systems with no synchronous connection to an interconnected system, such as some islands, the limits are more lenient. The mean value of the fundamental frequency measured over a period of 10 seconds must always be kept between the nominal value minus 15% and the nominal value plus 15%. It must also stay within a plus/minus 2% range 99.5% of the time, each week, meaning that it can only fall below 49% or exceed 51% during 0,5% of the week, [4].

As for the voltage variations, the mean of the RMS values measured for 10 minutes must stay within a plus/minus 10% range of the nominal value, 95% of the time, during each period of one week, [4].

It is also important to address the supply voltage unbalance. For every 10 minutes, the mean of the RMS values of the negative phase sequence component must stay within 0% and 2% of the positive phase sequence component, during 95% of each week, [4].

The international standard IEC 60850 establishes generic voltage limits for traction systems. Under normal operating conditions, the voltage value must be equal to or higher than the lowest permanent voltage, and equal to or lower than the highest permanent voltage. Under abnormal operating conditions, the voltage value can go as low as the lowest non-permanent voltage and as high as the highest non-permanent voltage. The limits for a typical case of an alternating-current supply with 25 kV nominal voltage are presented in Table 2.1, [5].

Table 2.1 - Supply voltage limits (root mean square (RMS) values), [5].

Lowest non-permanent voltage (V)	17500
Lowest permanent voltage (V)	19000
Nominal voltage (V)	25000
Highest permanent voltage (V)	27500
Highest non-permanent voltage (V)	29000

Regarding the values shown in Table 2.1, it is important to respect a few extra requirements. To begin with, the duration of voltages between the lowest permanent voltage and lowest non-permanent voltage must not be longer than two minutes, and the duration of voltages between the highest permanent voltage and highest non-permanent voltage must not be longer than five minutes. Plus, in a no-load condition, the busbar voltage for each substation must be lower or equal to the highest permanent voltage, [5].

Another important international standard to address is the IEC 61000-3-13. This is a technical report whose goal is to provide the principles to guide the coordination of the voltage unbalance between the different levels of voltage in a power system. To do this, it allocates emission limits for each installation, avoiding a high negative impact of the connection to the grid on the power quality, [6][7].

Another important international standard is the IEC 61000-3-6, whose goal is to establish harmonic limits for individual customers, to ensure that the voltage quality remains high. More specifically it establishes planning levels, which are targets that the customers must take into consideration when designing their systems, to be connected to medium-voltage (MV),

high-voltage (HV), and extra-high-voltage networks (EHV). These planning levels are represented in Table 2.2, as a percentage of the voltage, [8][9].

Table 2.2 - Voltage harmonic planning levels according to IEC 61000-3-6, [8][9].

Odd harmonics non-multiple of 3			Odd harmonics multiple of 3			Even harmonics		
Harmonic Order h	Harmonic Voltage %		Harmonic Order h	Harmonic Voltage %		Harmonic Order h	Harmonic Voltage %	
	MV	HV-EHV		MV	HV-EHV		MV	HV-EHV
5	5	2	3	4	2	2	1.8	1.4
7	4	2	9	1.2	1	4	1	0.8
11	3	1.5	15	0.3	0.3	6	0.5	0.4
13	2.5	1.5	21	0.2	0.2	8	0.5	0.4
$17 \le h \le 49$	$1.9 \cdot \frac{17}{h} - 0.2$	$1.2 \cdot \frac{17}{h}$	$21 < h \le 45$	0.2	0.2	$10 \le h \le 50$	$0.25 \cdot \frac{10}{h} + 0.22$	$0.19 \cdot \frac{10}{h} + 0.16$

Finally, it is necessary that the locomotives operating within the European Union also respect the parameters established in EN 50388 for the power factor. Table 2.3 represents these parameters regarding the inductive power factor, represented by lambda (λ) in the Standard. A TSI line consists of a rail line that belongs to the Trans-European Rail Network (TEN) and complies with the Technical Specifications for Interoperability (TSI). These are divided into various categories depending on the speeds and types of trains and can be both classical and high-speed (HS), [10].

Table 2.3 - Total inductive power factor (λ) of a train, modified from [10].

	Total inductive power factor λ of a train	
Instantaneous train power P at the pantograph (MW)	Category I and II of HS TSI lines [a]	TSI line category III; IV; V; VI; VII and Classical lines
$P > 2$	≥ 0,95	≥ 0,95
$0 \le P \le 2$	≥ 0.85	≥ 0.85

Analyzing the information in Table 2.3, for locomotives with a relatively high-power need of over 2 MW, the inductive power factor must be over 0.95, [10].

Also, EN 50388 has parameters for the locomotive capacitive power factor. During traction mode and standstill, within the voltage range of the lowest permanent voltage and the highest permanent voltage as established in IEC 60850, there are no limits for the capacitive power factor. However, when the voltage is between the highest permanent limit and the highest non-permanent limit, the locomotive shall not behave like a capacitor, which means that it cannot have a capacitive power factor, [5][10].

The overall power factor (λ) of the journey of a locomotive, including the stops, can be calculated using Equation 2.1. In this equation, the value of W_P represents the active energy in MWh, and the value of W_Q represents the reactive energy in Mvarh.

$$\lambda = \sqrt{\frac{1}{1 + \left(\frac{W_Q}{W_P}\right)^2}} \tag{2.1}$$

2.4 – Electrification involving transformers

One of the types of relatively basic solutions used in many countries is the employment of specially connected transformers in electric railway substations. This is currently the most widely used option because transformers are passive components that are relatively cheap. Among the different connections used, there is the single-phase connection, which is popular in Italy, France, and New Zealand, the V-V connection, which is popular in the UK, France, and Finland, the Wye-Delta Connection, which is popular in China, the Scott connection, which is popular in Japan, the LeBlanc connection, which is popular in Taiwan and the Modified-Woodbridge connection, which is popular in Japan, [11].

2.5 – Electrification involving power electronics

There are also active methods to face the challenges of projecting an electrified railway system. These resort to power electronics to mitigate the imbalance induced in the utility grid and the voltage drop on the feeder stations.

The use of static VAR compensators (SVCs) is currently the most established of these methods. The SVCs use thyristor-controlled reactors and thyristor-switched capacitors which creates the need for large filters to mitigate the effects of the additional harmonics that the thyristor switching introduces. They can regulate the catenary voltage magnitude but not the phase and frequency and therefore create the need for neutral sections separating the railway line so that the different voltages in different sections do not present an issue. The SVCs also present a passive catenary short circuit protection. Although the features of the SVCs are not particularly impressive, especially when compared to other power electronics solutions, these are relatively cheap and tend to do a good enough job in low-traffic railways. In Figure 2.4 there is a representation of an SVC with a Thyristor Switched Capacitor (TSC), a Thyristor Controlled Reactor (TCR), a harmonic filter, a mechanically switched reactor, and a mechanically switcher capacitor. [1][12].

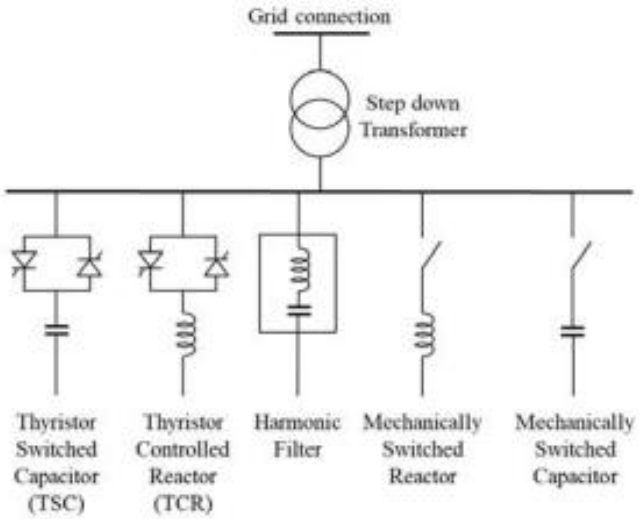

Figure 2.4 - Schematic use of an SVC in railways, [12].

An alternative to the use of SVCs is the use of static synchronous compensators (STATCOMs). These resort to switch-mode converters to compensate for the reactive power of single-phase transformers and filter the harmonics created by the railway loads. The stations are either connected to a single-phase overhead line or the three-phase grid, and their topologies can be a two-level H-bridge or a three-level H-bridge. Just like the SVCs, this solution does not make the regulation of catenary voltage phase and frequency possible and therefore there is a need for neutral sections too. It is interesting to note that both the SVCs and STATCOMs solutions have the advantage of being retrofittable to existing substations with very little service interruption. In Figure 2.5 there is a representation of the STATCOM technology being used in a substation, connected to the power grid side, [1][13].

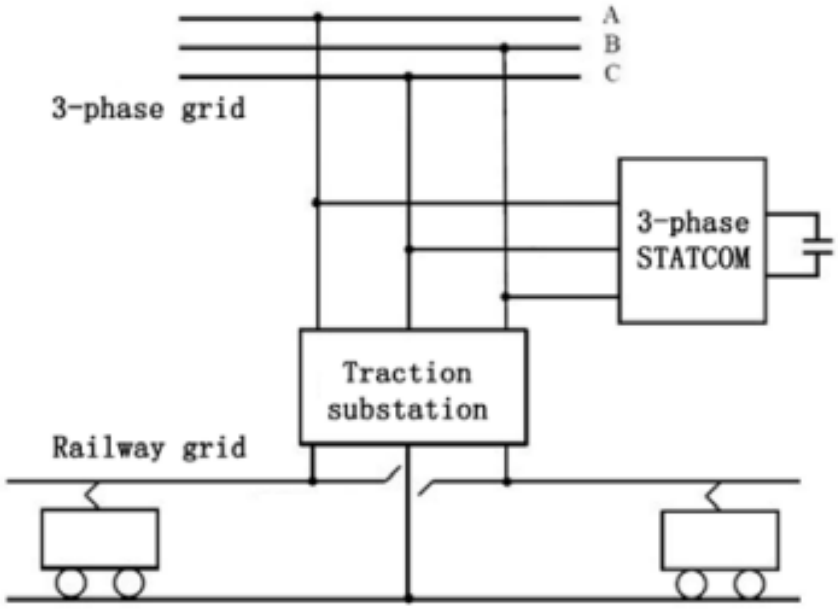

Figure 2.5 - Substation with STATCOM technology, [13].

2.5.1 – Full power converters

Another option is the use of full-power converters in feeder stations. This method draws a nearly sinusoidal current with a power factor very close to the unit. This means that the grid sees these feeder stations as balanced three-phase loads and that this converter can get power from lower voltage busses. This is a great development because in other solutions the potential locations of the substations are limited to places where a high-voltage transmission line passes. Furthermore, these converters have fully controlled currents on the three-phase side, which results in having the utility grid completely isolated from the tractions loads, which are nonlinear and unbalanced.

Another important feature of this solution is the possibility of controlling the voltage magnitude, phase, and frequency on the single-phase side (catenary). This creates the possibility of synchronizing this value with the output values of the full-power converters located in other feeder stations, which means that the overhead line of the railway can be continuous without the need for neutral sections spread across it. The possibility of monitoring the current on the single-phase side is also an advantage of full power converters, allowing the implementation of a catenary short circuit management scheme with a very low short circuit current and switchgear rating, [1].

There are different topologies when it comes to full power converters, mostly based on voltage-source inverters that convert the three-phase AC voltage to a DC and finally to a single-phase AC voltage. The back-to-back converter is a relatively simple topology, and its fault tolerance is very limited. In the event of a failure in a DC-link capacitor or a short circuit fault in a transistor of the H-bridges, this converter cannot operate. In Figure 2.6 there is a representation of a back-to-back converter with a three-phase bridge and a single-phase bridge [1].

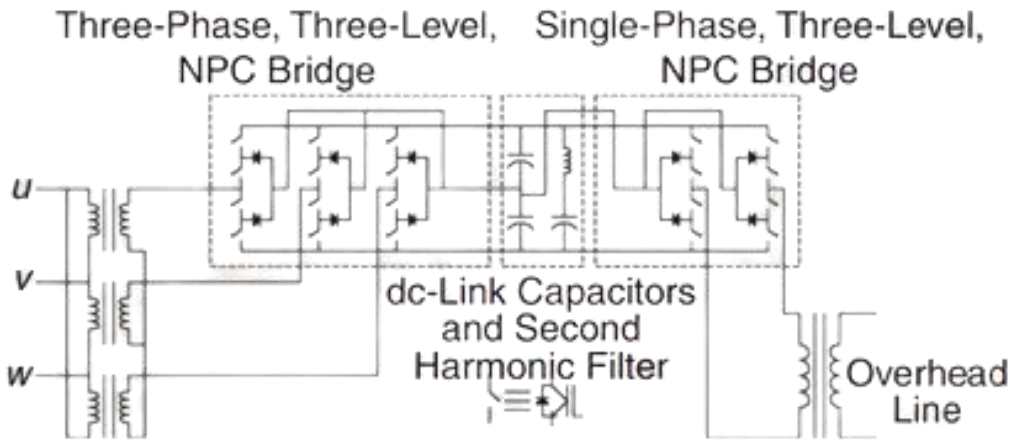

Figure 2.6 - Back-to-back converter, adapted from [1].

The single-phase cascaded H-bridge converter is another topology of full-power converters. This topology has multiple modules of back-to-back converters with their three-phase sides connected in parallel and their single-phase sides connected in series, which allows for a better fault tolerance and output waveform when compared to the back-to-back converter. The output waveform is formed by several layers which results in a reduction of the total harmonic distortion of the overhead voltage and the need for filters. There is also the advantage that in case of one of the H-bridges being faulty, the module in fault can be bypassed which means that the operation can continue if the remaining modules can cope with the voltage increase that results from the fact that one module is not performing its duty. In Figure 2.7 there is a representation of this topology, [1].

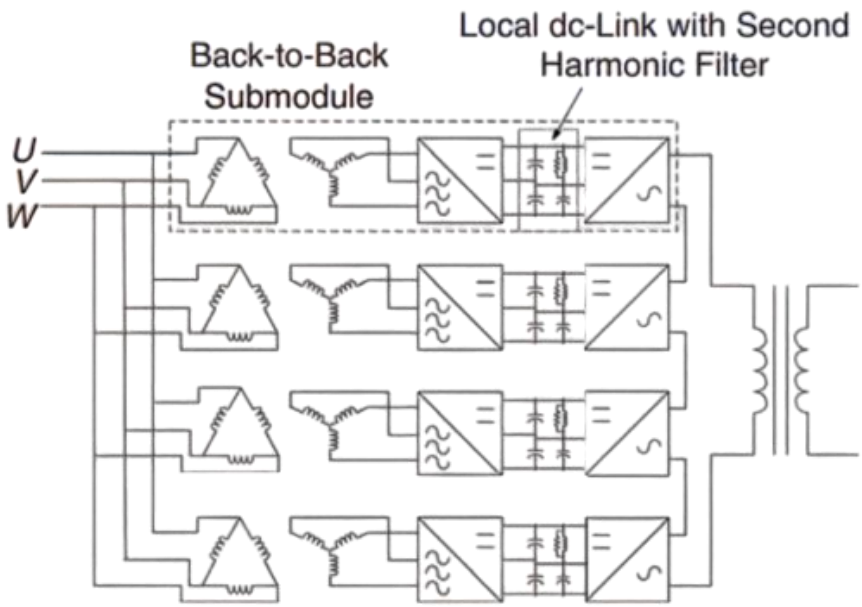

Figure 2.7 - Single-phase cascaded H-bridge with multiple DC-links, adapted from [1].

There are two different modular multilevel converter (MMC) configurations that can be used for railway static converters, the direct AC/DC, based on full-bridge submodules, represented in Figure 2.8, and the indirect AC/DC/AC, usually based on half-bridge submodules, represented in Figure 2.9. In both figures, SM represents the submodules, [1][14][15].

The MMC is a topology composed of arms where there is a large number of half-bridge or full-bridge submodules. To smooth the current waveforms, and limit the circulating current, each arm has a reactor. This topology has both the ability to deal with high voltages and its modularity as its two main benefits. It is currently one of the most interesting and promising solutions for the future of electrified railways, [1].

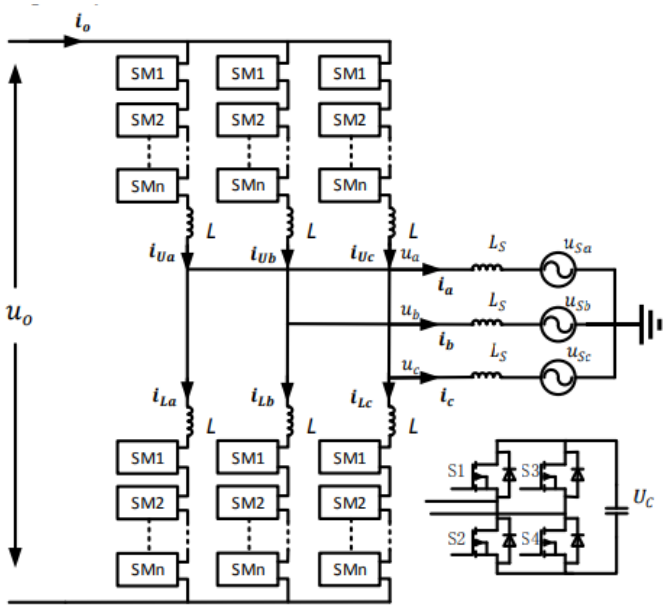

Figure 2.8 - Direct AC/AC MMC, [14].

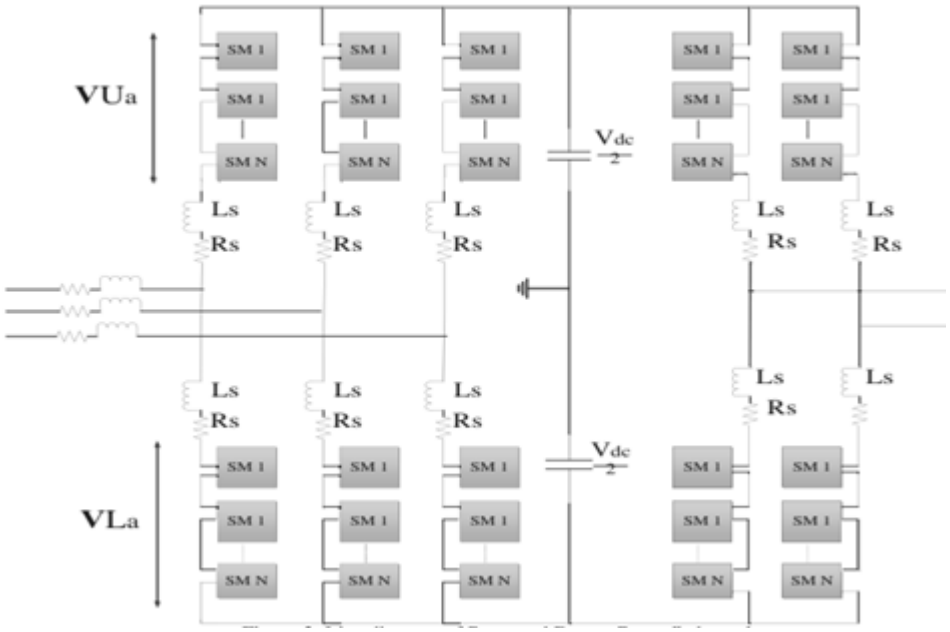

Figure 2.9 - Indirect AC/AC MMC, modified from [15].

2.5.2 – Hybrid solutions

In addition to the SVCs, the STATCOMs, and the full-power converters there are also the cophase and advanced cophase systems that consist in a hybrid solution that combines a STATCOM with a full-power static converter. The cophase system uses a single-phase-to-single-phase power converter and an impedance-matching YNvd transformer. In this solution, it is necessary to choose a winding ratio that potentiates a balanced three-phase side load when there is an equal magnitude and a 90º shift on the currents of the secondary winding. The main advantage of this hybrid solution over the STATCOM solution is the possibility of supplying active

power directly to the load. Figure 2.10 shows a representation of the cophase system, where there is a traction transformer (TT) and a cophase compensation device (CPD). In Figure 2.10, the latter is composed of a back-to-back converter, a high-voltage matching transformer (HMT), and a traction matching transformer (TMT) [1][16].

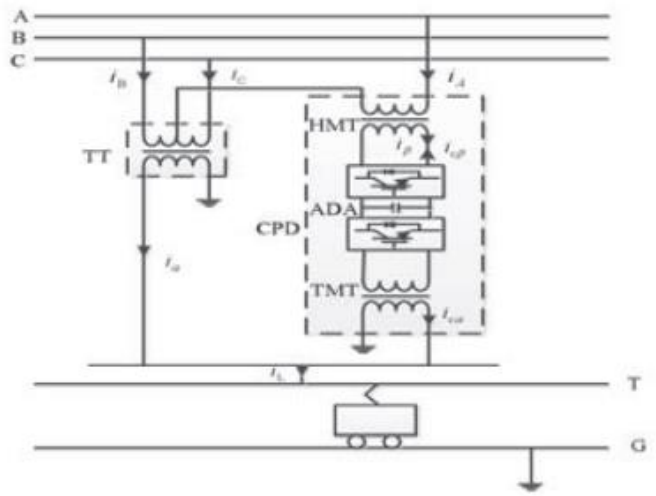

Figure 2.10 - Cophase system, [16].

Research into this area has led to the development of the advanced cophase system, which is an improved version of the cophase system. In the advanced cophase system, the YNvd transformer is replaced by one single-phase transformer and one three-phase transformer. Both the cophase and advanced cophase power supplies can maintain the load balance on the three-phase side, allow the omission of neutral sections in the railway network, and make the regulation of catenary voltage and phase possible. Plus, it features harmonic compensation, passive catenary short circuit protection, and passive filters of small size. In Figure 2.11 there is a representation of the advanced cophase system, [1][17].

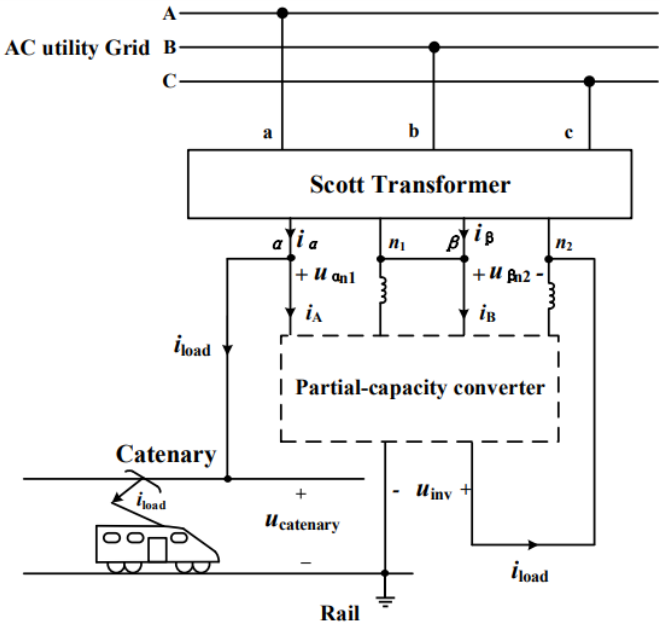

Figure 2.11 – Advanced cophase system, [17].

It is important to address that inverters currently on the market can only take certain levels of voltage. Because in typical railways the RMS value of the voltage is around 25 kV, the peak value is around 35 V. This value is very high, creating the need for the use of multiple inverters connected in a substation, distributing the voltage, and allowing for a healthy working condition for the inverters.

2.6 – Conclusions

As a conclusion, there are many ways and technologies capable of feeding power to the railways. Each has its own advantages and disadvantages. While some have been applied for a long time, others, namely the ones that use power electronics, are relatively new and will be subject to further studies and likely introduced in more railways.

The increasingly stricter standards to make the process of supplying power to the railways more efficient for all parties involved makes the development of these technologies an important area. When designing a railway line and its substations, it is important to pick solutions that meet these standards in a cost-efficient and safe manner, given the railway´s characteristics, regarding, among others, size, locomotives type, traffic, and distance between substations.

Chapter 3

Load models and static characteristics

This chapter discusses different possibilities for representing a locomotive in simulations and shows some preliminary simulations regarding the impact of the relative position in the catenary and power factor of a locomotive.

3.1 – Locomotive models in Simulations

With the goal of better understanding how the catenary voltage changes with different conditions, a few simple preliminary studies were conducted. To better understand these studies, it is important to know how the locomotives can be represented in calculations and simulations. The three different representations are shown in Figure 3.1, Figure 3.2, and Figure 3.3.

In Figure 3.1 the locomotive is represented by an impedance, with a value for the resistance and a value for the inductance. This representation is very simple and does not allow the simulation of situations when the train is braking and, consequently, regenerating energy. This happens because these moments are characterized by current flowing from the locomotive to the catenary. As the impedance cannot be negative, it only allows for simulations where the current flows from the catenary to the locomotive.

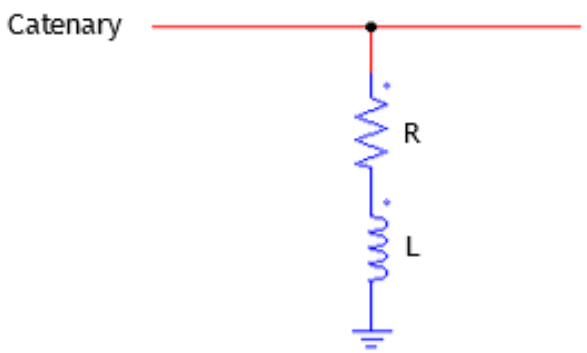

Figure 3.1 - Representation of a locomotive through an impedance.

In Figure 3.2 the locomotive is represented by a current source. Although this representation is still not ideal, because the catenary voltage varies, and consequently it does not allow the direct control of the load´s power, it does allow the simulation of situations when the locomotive is regenerating, by changing the direction of the current flow.

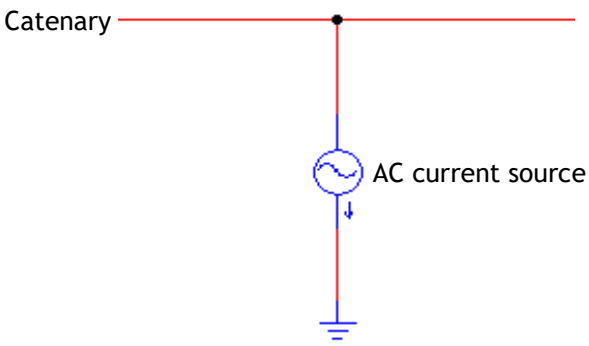

Figure 3.2 - Representation of a locomotive through a current source.

In Figure 3.3 the locomotive is represented by a PQ load. This is the best representation as it is the one that gets closer to reality, allowing the control of the active and reactive power consumed or regenerated by the locomotive. The only downside of this representation is that some of the simulation software available does not have this model, although it can be implemented easily, but turns the simulation much longer.

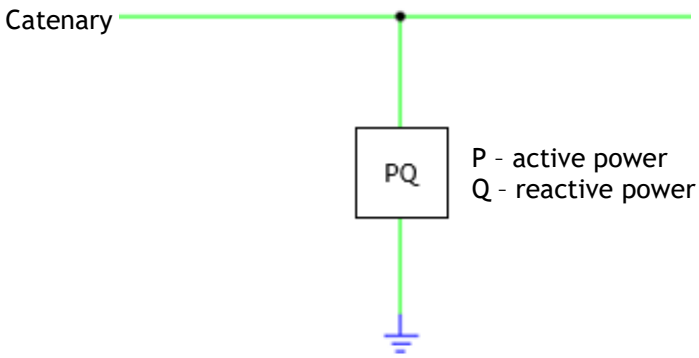

Figure 3.3 Representation of a locomotive through a PQ load.

3.2 – First study: distance influence

Due to the simplicity of these preliminary studies, an impedance was used to module the locomotive as it is enough to achieve the proposed goals. In the first and second studies, a portion of a railway connecting a substation and a neutral section was considered, as shown in Figure 3.4.

The goal of the first study is to understand how the distance between the locomotive and the substation affects the voltage in the point connecting the catenary and the locomotive. For this, it was considered a typical value of 25 kV with phase 0 for the voltage in the substation

(V1) and a distance between the substation and the neutral section of 40 km. Therefore, the distance between the locomotive and the substation can vary between 0 km and 40 km. The resistance of the catenary considered was 0.1 Ω/km and the inductance was 1 mH/km. As for the locomotive, it was considered a power consumption (S) of approximately 6 MVA. The impedance used to model the locomotive was calculated using Equation 3.1 and considering a voltage value (V) of 25 kV.

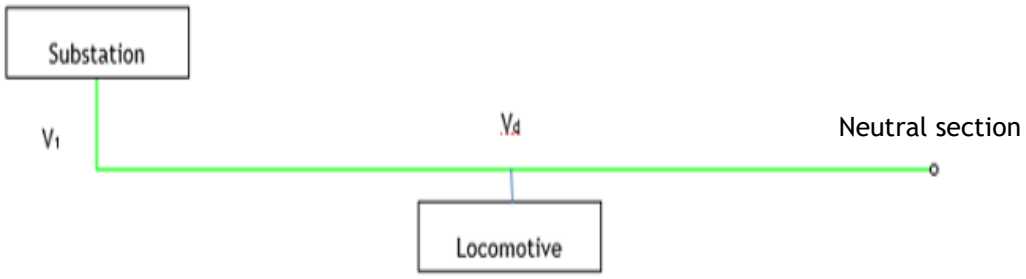

Figure 3.4 - Representation of the conditions in which the first and second studies were conducted.

$$Z_L = \frac{{V_L}^2}{S} \tag{3.1}$$

The value obtained was 104 Ω. The power factor was kept at 1 for this study, meaning that there is no inductance. In any given moment the value of V_d is given by Equation 3.2, where the "d" represents the distance between the substation and the locomotive.

$$V_d = \frac{V_1 * Z}{Z + d * Z_{catenary/km}} \tag{3.2}$$

A script was developed taking into consideration these values and equations, and the result for $|V_d|$ is represented in Figure 3.5.

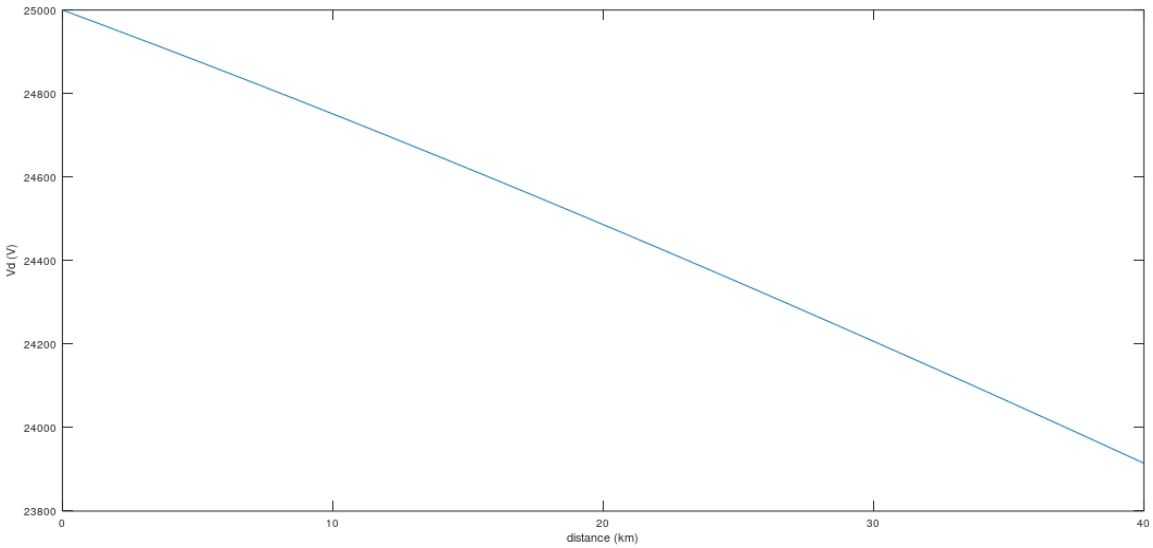

Figure 3.5 - Voltage variation with the distance between the locomotive and the substation.

By analyzing Figure 3.5, it is easy to conclude that the Vd voltage drops as the distance between the locomotive and the catenary increases. This results from an increasingly higher

catenary impedance. More specifically, it drops from 25 kV at 0 km to around 23.9 kV at 40 km. The result highlights one of the main problems of supplying locomotives with one substation at a time, with different sections of the catenary separated by neutral sections. A lower voltage means higher currents supply the locomotive with the required power, which is not ideal. Nevertheless, all the voltage values obtained are still well within the permanent limits established by IEC 60850, [5].

3.3 – Second study: power factor influence

A second study was done, again taking into consideration the representation shown in Figure 3.4. This time the goal was to understand the impact of the power factor of the locomotive on the Vd voltage value. To achieve this, the distance between the substation and the locomotive was fixed at 40 km, as it is the worst-case scenario from the previous study. The values considered for V1, the resistance and inductance of the catenary, and the module of the impedance of the locomotive were the same as in the previous experiment. The only difference is that this time, the impedance of the locomotive is not fully resistive, as the power factor varies between 0.8 and 1. The result is shown in Figure 3.6.

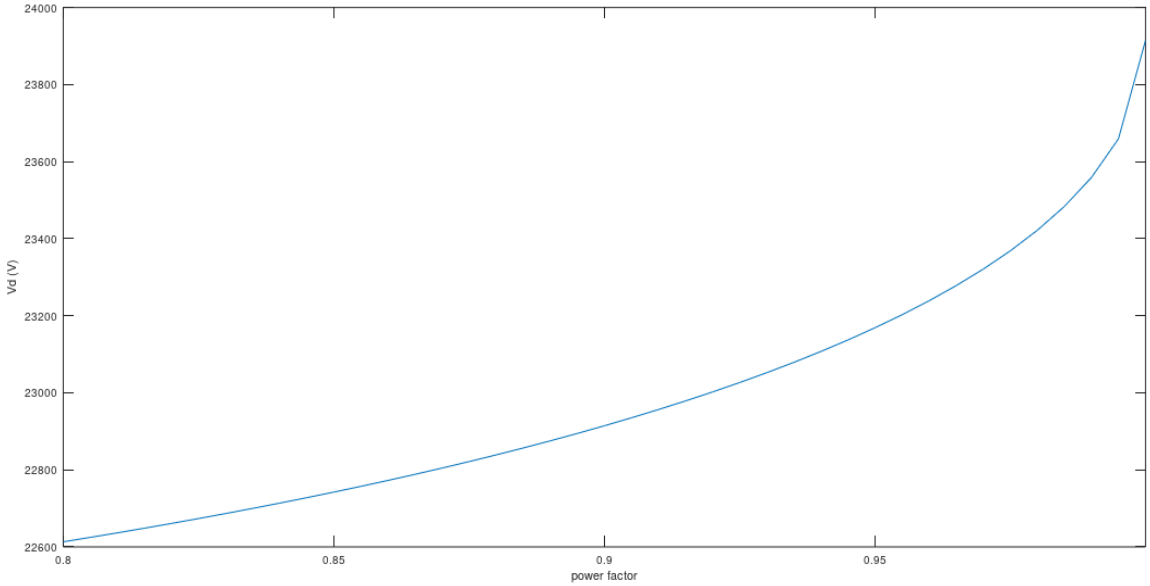

Figure 3.6 - Voltage variation with the power factor of the locomotive.

Analyzing Figure 3.6, the conclusion is that the voltage value grows exponentially with the power factor increase. As a result, it is important that locomotives do not consume too much reactive power in comparison to active power so that the power factor remains high, and the voltage drop is not too significant. It is also interesting to notice that the value obtained for a power factor of 1 is equal to the one obtained in the previous study for 40 km, as these represent the same situation (distance of 40 km and power factor of 1). In this study, the relatively low power factor values were used to better represent the issues associated with it. In real situations, locomotive power factors tend to be above 0.95, as established in EN 50388.

The voltage values obtained are all well within the permanent limits established by IEC 60850, [5][10].

3.4 – Third study: bidirectional feeding

To have an idea of the impact of not having a neutral section, and instead having a second substation supplying the locomotive at the same time, a third study was conducted. A representation of the conditions of this study can be seen in Figure 3.7.

The value of the impedance used to represent the locomotive was kept at 104 Ω, and the power factor at 1. The values of resistance and inductance of the catenary were maintained, and so was the value of V1. The value of V2 was placed at 25 kV and phase 0, just as V1, so that the results are simple and easy to analyze. Since in the previous experiment the distance between the substation and the neutral section was 40 km, in this study the distance between substations was fixed at 80 km.

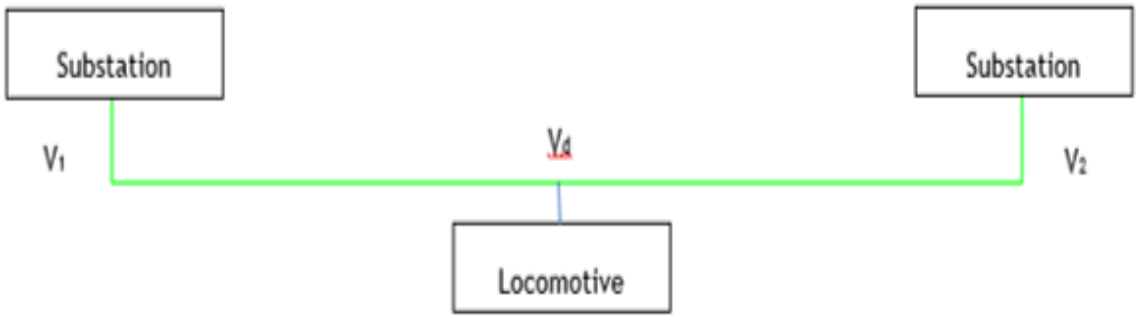

Figure 3.7 - Representation of the conditions in which the third and fourth studies were conducted.

At first, the goal was again to discover the value of Vd as a function of the distance between the locomotive and the first substation. This value can be obtained by using Equation 3.3.

$$V_d = \frac{V_1 * Z//Z_2}{Z_1 + Z//Z_2} + \frac{V_2 * Z//Z_1}{Z_2 + Z//Z_1} \tag{3.3}$$

For a better understanding of Equation 3.3, it is important to address the calculation of Z1 and Z2, which represent the impedance of the catenary between the first substation and the locomotive, and between the locomotive and the second substation, respectively. Equations 3.4 and 3.5 show this calculation, where "d" represents the distance between the first substation and the locomotive.

$$Z_1 = d * Z_{\frac{catenary}{km}} \tag{3.4}$$

$$Z_2 = (80 - d) * Z_{\frac{catenary}{km}} \tag{3.5}$$

With the described conditions in mind, a script was developed. The results obtained are represented in Figure 3.8.

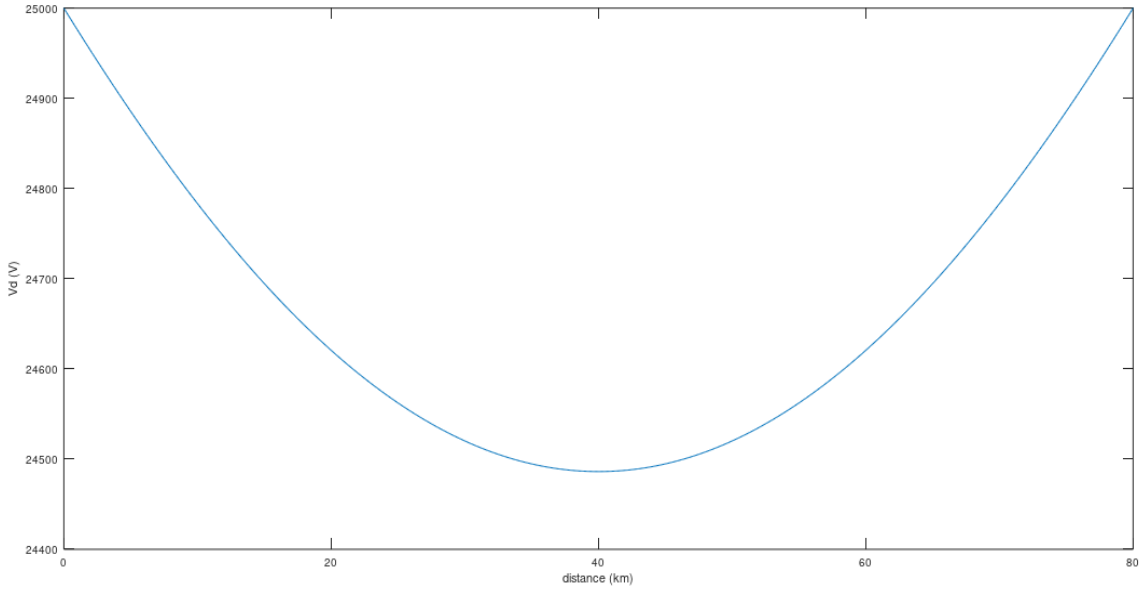

Figure 3.8 - Voltage variation with the distance between the locomotive and the first substation.

3.5 – Fourth study: power sharing

Using the same conditions, a fourth study was conducted. This time, the goal is to understand the apparent power that the locomotive consumes for the different distance values. In addition, this power was divided between the two substations, to understand how much each substation is contributing to the overall power value for any given distance. For this study, the power factor was kept at 1. To obtain the apparent power supplied to the locomotive, Equation 3.6 and Equation 3.7 were used to obtain the currents flowing to the locomotive from the first and second substations, respectively.

$$I_1 = \frac{(V_1 - V_d)}{Z_1} \tag{3.6}$$

$$I_2 = \frac{(V_2 - V_d)}{Z_2} \tag{3.7}$$

Having these values, it becomes possible to obtain the power contribution of the first and second substation, neglecting the voltage drops, by using Equations 3.8 and Equation 3.9, respectively.

$$S_1 = V_d * I_1^* \tag{3.8}$$

$$S_2 = V_d * I_2^* \tag{3.9}$$

The total apparent power consumed by the locomotive is given by Equation 3.10.

$$S = S_1 + S_2 \tag{3.10}$$

With these equations in mind, a script was developed, and the results obtained are presented in Figure 3.9.

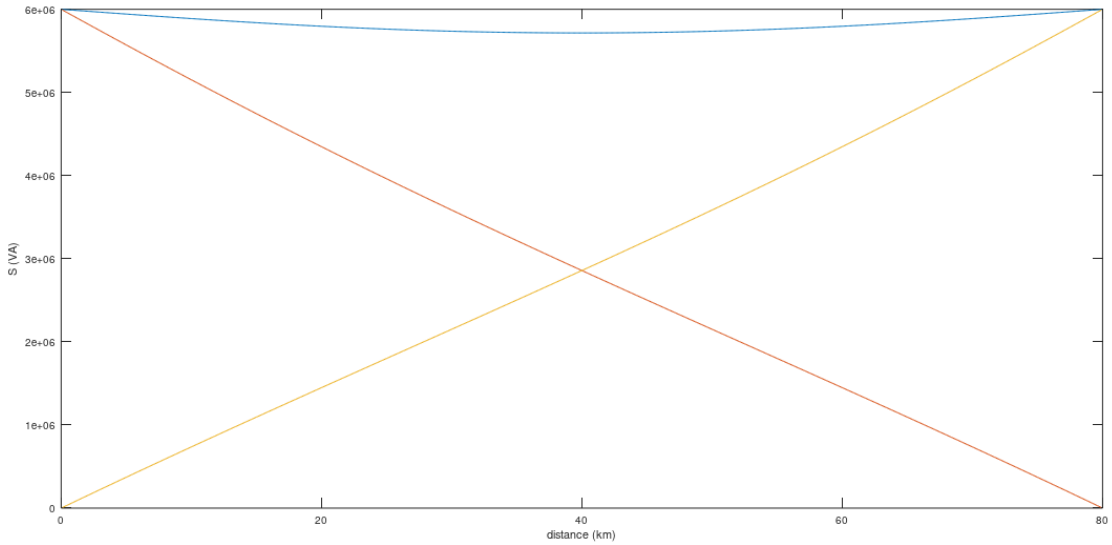

Figure 3.9 - Apparent power consumption varies with the distance between the locomotive and the first substation.

In Figure 3.9, the blue line represents the total consumption of apparent power, the red line represents the contribution of the first substation and the yellow line represents the contribution of the second substation. It is visible that the apparent power consumed stays close to 6 MVA throughout the entire length of the catenary section. Nevertheless, when the locomotive is passing the substations (0 km and 80 km), the apparent power is higher and when it is further away from them (40 km) it is lower. Plus, at the 0 km point, the power is fully supplied by the first substation. As it advances, the contribution of the first substation decreases, and the contribution of the second substation increases. At the 40 km point, the contributions from both substations are equal. Finally, at 80 km the situation is the opposite of the one at the 0 km point. This time, the power is fully supplied by the second substation.

If for any reason it is necessary to change the power contribution of each substation to the locomotive, this can be achieved by altering the magnitude and phase of the voltage in one or more substations. The possibility to control these values is one of the main reasons why power electronics are gaining an increasingly bigger presence in railway substations.

3.6 – Conclusions

These four studies give a simplified overview of the way certain parameters change in different conditions. The main conclusions are that the voltage tends to drop the further away a locomotive is from the substations, and this drop is more significant when the power factor of the locomotive is lower. It can also be concluded that in a situation where more than one

substation is supplying the same locomotive, the substation closer to it tends to supply a bigger percentage of the total power.

Nevertheless, it is important to address that in real situations there might be more than two substations supplying the locomotive at any given moment, and more locomotives passing through the same section of the catenary, which does not happen in these studies

Chapter 4

Design and test of a railway substation

In this section, the goal was to develop and test a model for a traction substation that makes it possible to feed a maximum of at least 20 MW to the catenary. As a secondary goal, the substation also enables the transit of power from the catenary to the power grid, which happens when the trains are braking and, therefore, regenerating energy. This substation is connected to a three-phase power grid on one side, and the catenary on the other side. Considering the focus of this document on the modernization of the energy supply in electrified railways, the substation is based fully on power electronics converters.

Given the previously stated solutions available, it was decided to divide the development and testing of the substation into two components. The first one is the three-phase AC/DC conversion, which connects the power grid to a DC-link and the second one is the single-phase DC/AC conversion, which connects the DC-link to the catenary.

4.1 – Design of the three-phase AC/DC conversion module

To begin with, some decisions had to be taken regarding the topology of the converter to be developed. After a careful analysis of the possibilities, an NPC-based solution was picked. The diagram of this topology used is represented in Figure 4.1.

This solution could not be used in a real-world situation without transformers, because of the limitations associated with the transistors´ voltage tolerance. As an example, the IGBT FZ1800R45HL4, fabricated by Infineon, one of the transistors with higher voltage rating currently on the market, tolerates voltages of up to 4.5 kV, which is nowhere near enough to make this topology work. Nevertheless, it was selected due to its convenience regarding the simulation efficiency, as well as being able to show the basic principles of the AC/DC conversion and its control. A more realistic MMC topology was considered, but the extensive simulation times and control difficulties that are not the subject of this work make it less interesting for

this section. Plus, the contact and study of the MMC topology will be done later anyway, in the DC/AC converter, [18].

Another important decision was the voltage value desired for the DC-link. As previously mentioned, the maximum permanent value of the AC voltage in the catenary is defined as 27.5 kV, according to the international standard IEC 60850. Taking this value as an aim for the desired catenary voltage, this results in a peak voltage of 38.89 kV, as shown by Equation 4.1. Considering this result and to allow for a good margin, a value of 42 kV was decided for the voltage value of the DC-link, [5].

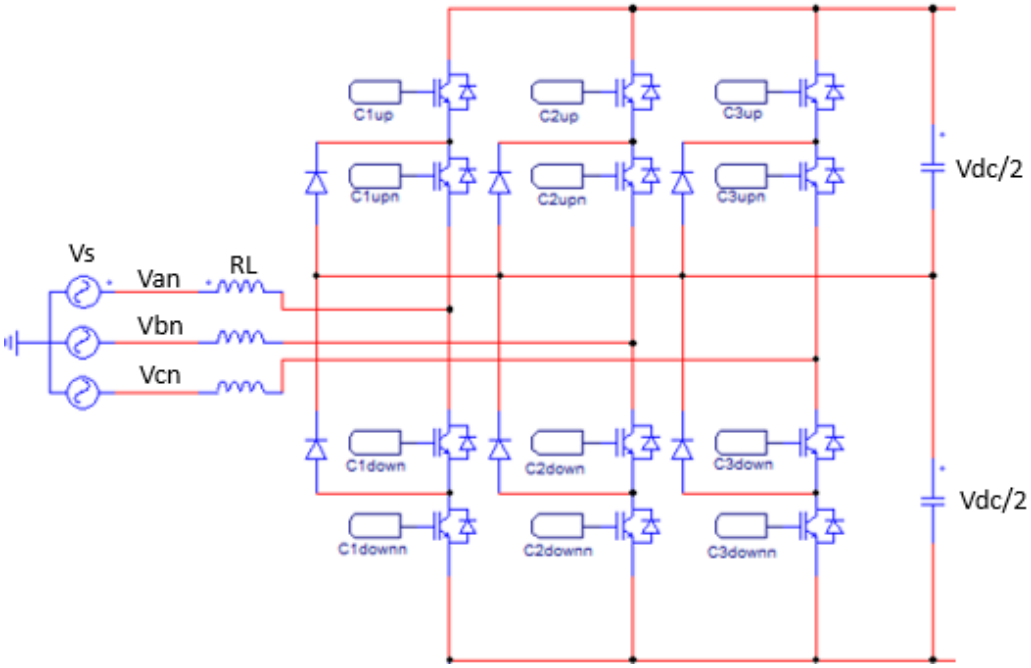

Figure 4.1 - AC/DC NPC converter.

$$V_{peak} = 27.5k * \sqrt{2} = 38.89\ kV \tag{4.1}$$

To achieve this voltage in the DC-link, it was calculated a voltage for the primary side of the converter, as shown in Equation 4.2. A 20% margin was given to this value, which means that the primary voltage was fixed at 26 kV. As a result, in a real-world application, it would be necessary to incorporate a transformer capable of altering the voltage value of the power source, which in this case is the power grid, to 26 kV so that it is compatible with the developed converter.

$$V_{sLL} = \frac{42k}{1{,}35} * (1 - 0.2) = 26\ kV \tag{4.2}$$

Regarding the control circuit, it was developed based on a voltage-oriented control (VOC), as presented in the following figures and equations. The two signals generated by the control are produced considering the base equations for the vectorial control of an AC/DC three-phase converter. These are Equation 4.3 and Equation 4.4, where L is the inductance value of the AC connecting inductor, R is the parasitic resistance of this inductor and ω is the grid angular frequency.

$$V_{cd} = R * I_{sd} + L\frac{dI_{sd}}{\mathrm{dt}} - \omega L * I_{sq} + V_{sd} \quad (4.3)$$

$$V_{cq} = R * I_{sq} + L\frac{dI_{sq}}{\mathrm{dt}} + \omega L * I_{sd} + V_{sq} \quad (4.4)$$

First, the values of the voltages of the three phases of the grid connecting end are taken and used to obtain a value of theta, using an abc/αß block and an atan2 block, as shown in Figure 4.2. It is worth mentioning that the theta value could also be obtained using a PLL block, a more common solution is power electronics control, [19].

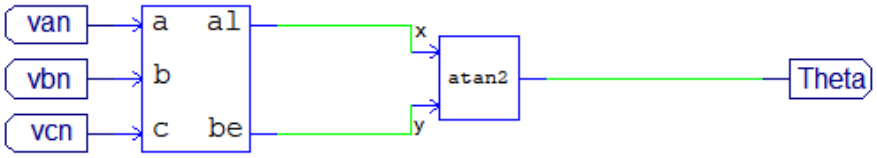

Figure 4.2 - Obtention of theta.

This value of theta is then used to transform the values of the voltage and current taken in each phase from a stationary phase coordinate system (abc) to a rotating coordinate system (dq0), through direct-quadrature-zero transformation blocks, as shown in Figure 4.3, [19].

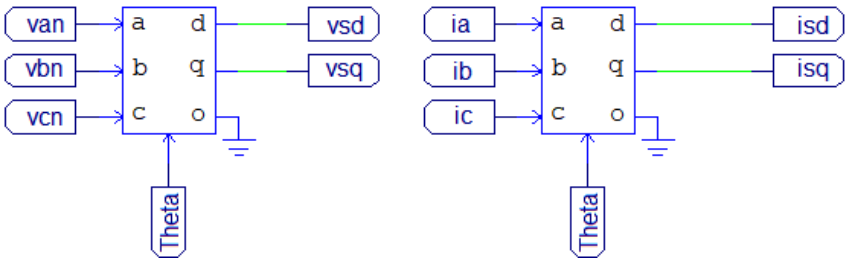

Figure 4.3 - ABC-dq0 transformation.

Simultaneously, the value of the DC-link voltage is being measured and used to obtain a value for a reference current for isd, which leads to a 42 kV voltage in the DC-link. The reference current for isq is taken as 0 because it is responsible for controlling the reactive power, and since the desired power factor is unitary, the reactive power must be non-existent. This process is shown in Figure 4.4, [19].

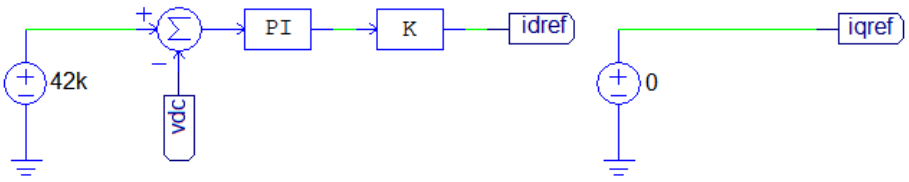

Figure 4.4 - Idref and Iqref generation for unitary power factor.

The mentioned values are then used to generate three signals to be used in the control of the three arms of the converter, through a typical vectorial control process involving

multiple operations, and a transformation back from the rotating coordinate system to the stationary phase coordinate system. The overall process is represented in Figure 4.5, [19].

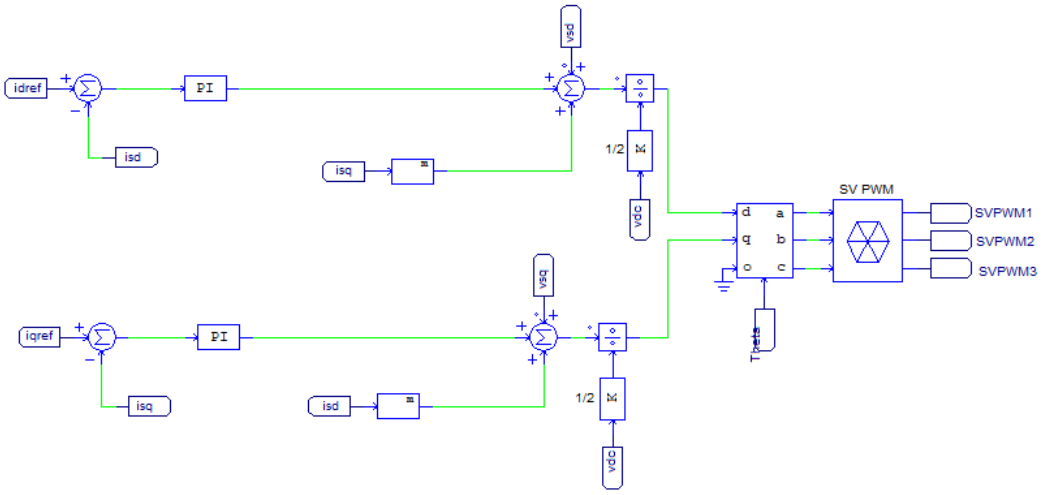

Figure 4.5 - Control signals generation

Finally, the signals are modulated using the space vector modulation (SVM) technique and a double modulation wave carrier based PWM. While in a normal converter topology only one carrier wave would be used, in this situation there are two triangular waves with a duty cycle of 0.5 and a peak-to-peak value of 1. Given that this is an NPC topology, one of the signals has a DC offset of -1, appearing between 0 and -1, and the other has a DC offset of 0, appearing between 0 and 1. The switching frequency selected is 2 kHz. This process is represented in Figure 4.6, [20].

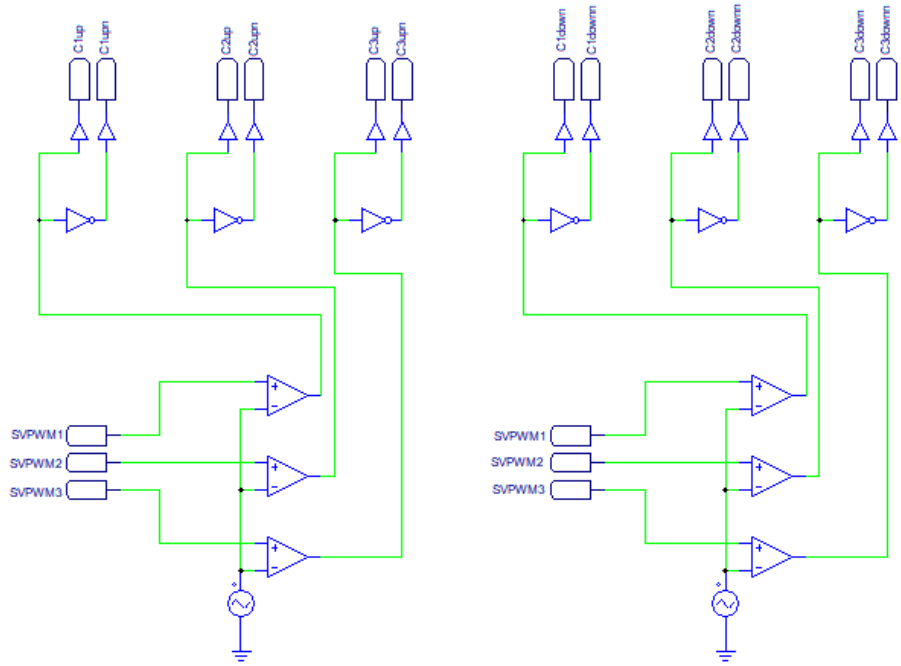

Figure 4.6 - Modulation

In NPC topologies the balancing of the voltage in the capacitors is an important aspect. However, since it is not an objective of this work, it was not addressed. In the same way of reasoning the dead time between complementary switches was also not implemented in this model, [20].

4.2 – Testing of the three-phase AC/DC conversion module

The developed converter was subject to a series of tests, to verify its ability to achieve the desired goals of the project, and better understand its strengths and limitations. In a real-world scenario, starting a converter of this calibre would require a pre-charge circuit, to avoid excessive current values flowing suddenly through the equipment. This would consist of blocking the control pulses and placing switches in the lines connecting the grid to the converter, turning this connection off. At the same time, a parallel connection from the grid to the converter, with resistors, to control the current, is active, but also with switches that can turn it off later. This way, the DC-link capacitors are charged in a slow and controlled way. After these capacitors reach the desired voltage, the control system, and the normal connection to the grid start operating, and the lines with resistors are turned off. To simulate the effect of this pre-charge circuit, an initial value of 30 kV was placed in the DC-link capacitors. The first test was done using a DC current source on the secondary end of the conversion module, to simulate the current required to feed power to the catenary. The value chosen for the current source was obtained using Equation 4.5 so that the power passing through is the maximum expected of the substation, which is 20 MW.

$$I_{dc} = \frac{P_N}{V_{dc}} = \frac{20M}{42k} = 476.19\ A \tag{4.5}$$

The main goal of the first test was to show that the conversion process does meet the requirements established by the previously mentioned European Standard EN 50160 regarding supply voltage unbalances and by the international standard IEC 61000-3-6 regarding harmonics. As a secondary goal, this test also looks to show the conversion module´s ability to deliver a voltage of 42 kV on the DC-link and, consequently, 20 MW of power [4][7].

In Figure 4.7 there is a representation of the voltages in each of the three phases of the grid connecting side of the converter, between a simulation time of 0.73 and 0.765 seconds. Although the figure does not give a precise viewing of the voltage balance and a more detailed analysis would be required to confirm this, it does show an apparent balance between them. Anyway, it was previously seen that a power electronics converter is seen by the power grid as a balanced load, keeping the voltages balanced and respecting EN 50160. For the same period, Figure 4.8 shows the simple voltage value on phase A, on top, and the line-line voltage value measured between phase A and phase B, at the bottom. The line-line voltage value reaches higher values, as expected, [1][7].

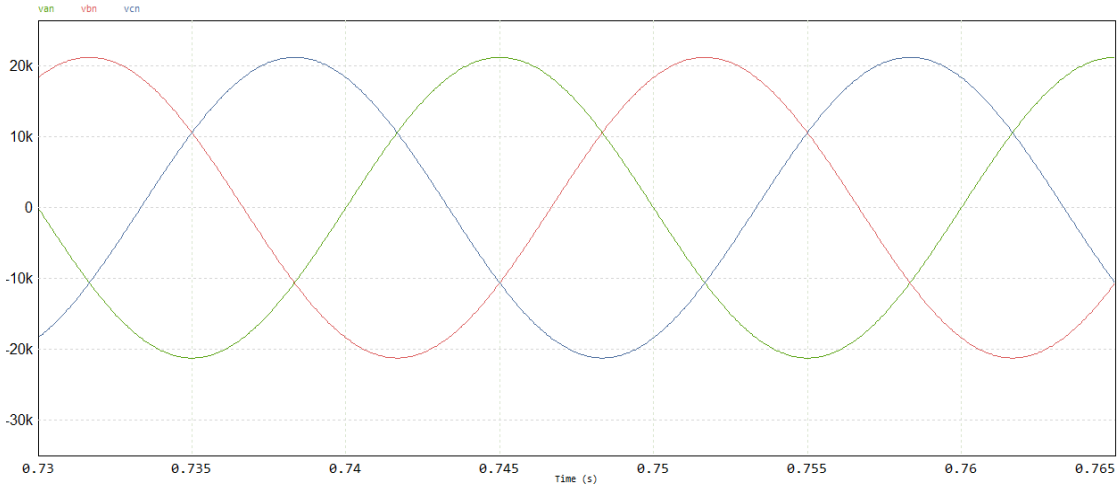

Figure 4.7 - Grid connecting side voltage values.

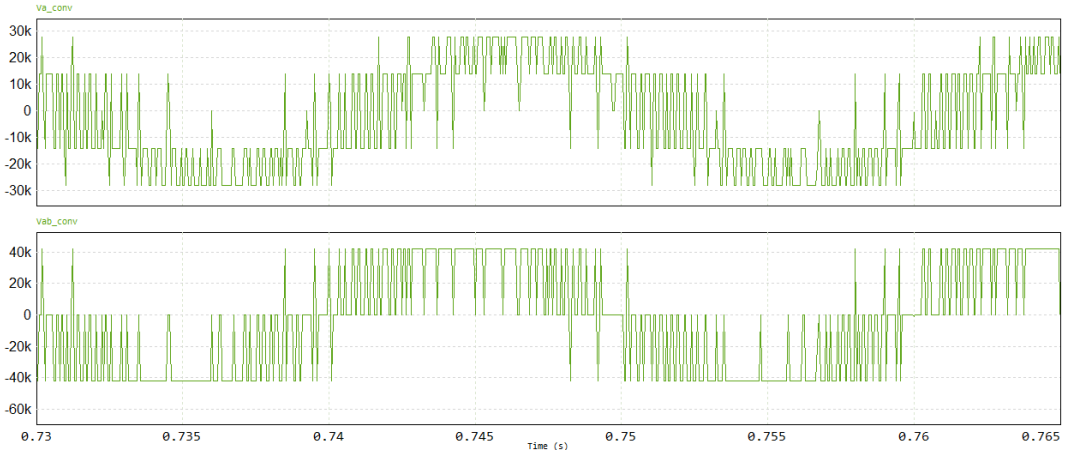

Figure 4.8 - Simple and line-line voltage values at the converter.

For the same period, the wave of the current in phase A of the grid-connecting end was taken and represented in Figure 4.9. Analyzing it, is apparent that it is not a perfect sinewave and does have harmonic distortion, as expected. Using the THD function of PSIM, the total harmonic distortion of the wave was calculated as 0.0216. This is a very low value and does respect the requirements of IEC 61000-3-6 in this regard, by a comfortable margin, [8].

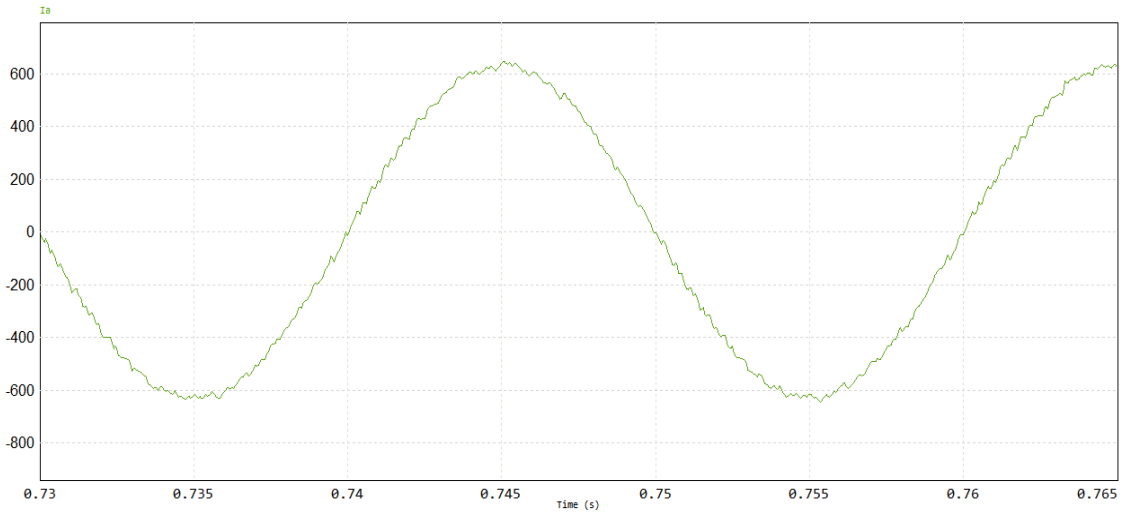

Figure 4.9 - Current in phase A in the first test.

The voltage in the DC link can be seen in Figure 4.10, for the total length of the simulation. Since the pre-charge process was not simulated, an initial capacitor voltage of 30 kV was used. Is it noticeable that after a period of transition of about 0.7 seconds, it stabilizes at 42 kV, as expected. It is also interesting to notice that, in this case, the control system developed manages to achieve the desired results without allowing the DC-link voltage to overshoot too much, with its maximum value being around 43 kV.

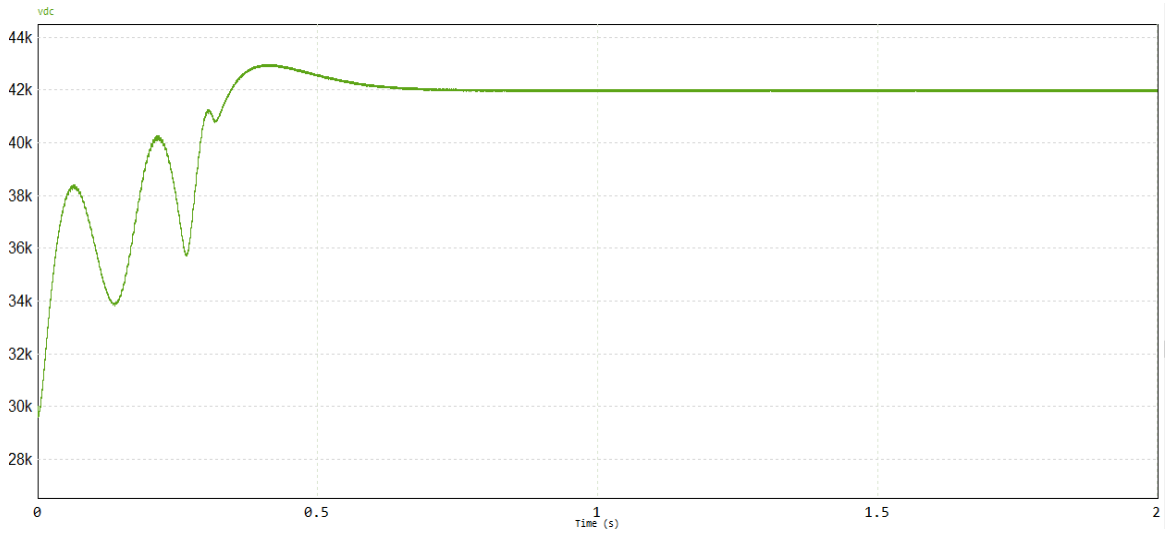

Figure 4.10 - DC link voltage in the first test.

Finally, there is the power passing through the conversion module represented in Figure 4.11. Just like the DC voltage it goes through a transitory period before stabilizing around 20 MW, as expected given the values of the voltage and current on the DC-link. Since the current is always the same, as it is provided by a source, the power value is fully dependent of the voltage value and takes the same time to stabilize.

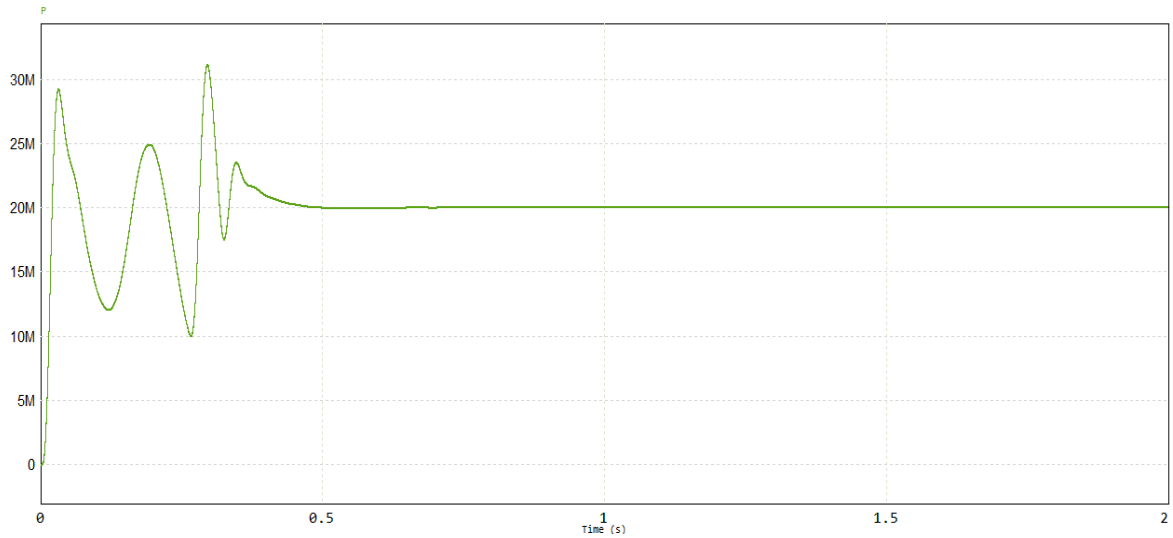

Figure 4.11 - Power supplied in the first test.

The second and third tests have the goal of showing the behavior of the conversion process when faced with a sudden change of conditions, namely a change in the power required

to feed the trains passing in the catenary. To simulate this, a current step module was used.

Regarding the second test, the initial value of the current was 0 A, simulating a situation where 0 MW are fed to the catenary. At the timestamp of 0.5 seconds, the value suddenly changes to 476.19 A, representing a situation where 20 MW are being fed to the catenary. It is important to mention that this test is ideal and very extreme, as an increase in power demand from 0 MW to 20 MW is not expected to happen in a real-world situation, particularly in a step way, as it happens in this case.

In Figure 4.12 there is a representation of the voltage in the DC-link between 0.4 and 1.5 seconds. Before that, the voltage value stabilizes at around 42 kV as expected, near 0.4 seconds. Compared with the scenario of the first simulation, where there is a load, the time the voltage takes to stabilize is lower, but the overshoot is slightly higher reaching approximately 44 kV (not shown in the figure). At 0.5 seconds, a big instability is caused by the sudden increase in the current value, resulting in a drop in the voltage value before stabilizing once again at around 42 kV, near 0.8 seconds. In this situation, the voltage drops a lot, which is a negative aspect, but the time it takes to get back to the target value is relatively short, which is a positive one. A smaller magnitude of the step and a lower gradient would both contribute to a much smoother dynamics of the DC-link voltage.

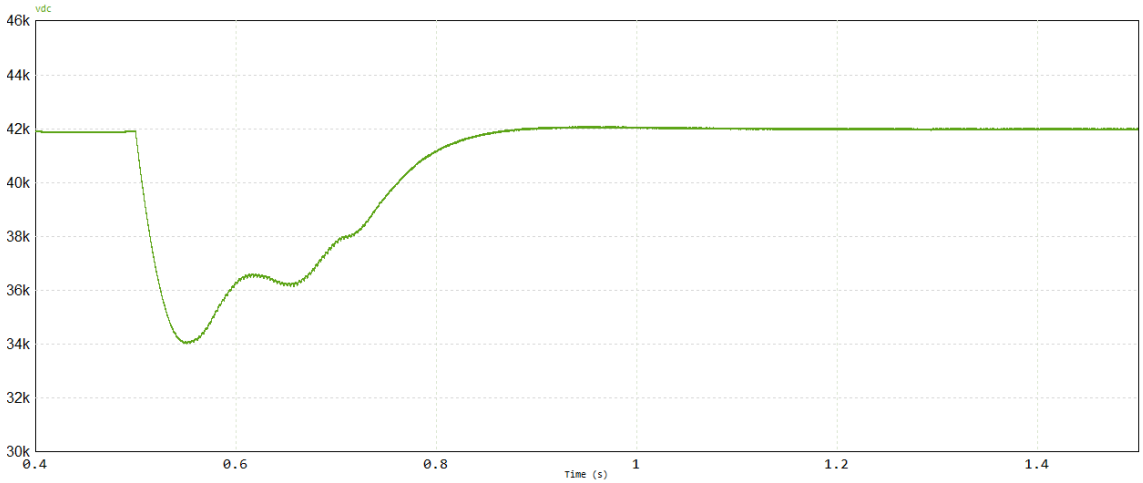

Figure 4.12 – DC-link voltage in the second test.

Another interesting representation is the currents flowing on the three-phase side, represented in Figure 4.13 for the same period of Figure 4.12, between 0.4 and 1.5 seconds. These are initially very close to 0 A, as this is a no-load situation. The sudden increase in current on the DC-link at 0.5 seconds results in an increase in the current on the tree-phase side. After this increase there is some minor instability before the current reaches a relatively stable state again, once the converter finds a stable operating state.

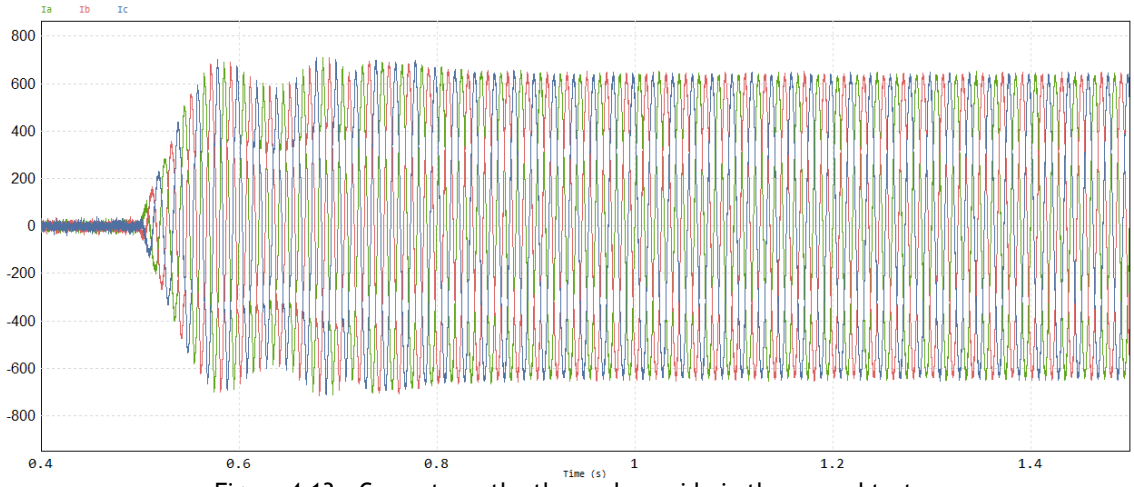

Figure 4.13 - Currents on the three-phase side in the second test.

A similar behaviour is seen in the power supplied, represented in Figure 4.14 for the same period between 0.4 and 1.5 seconds. Before that, there is some instability natural of the final stage of the pre-charge process, before the value stabilises at around 0 MW, as expected, because there is no load. At 0.5 seconds, the instability caused by the sudden increase in the current value occurs, but it takes little time before stabilizing once again, this time at around 20 MW, as expected.

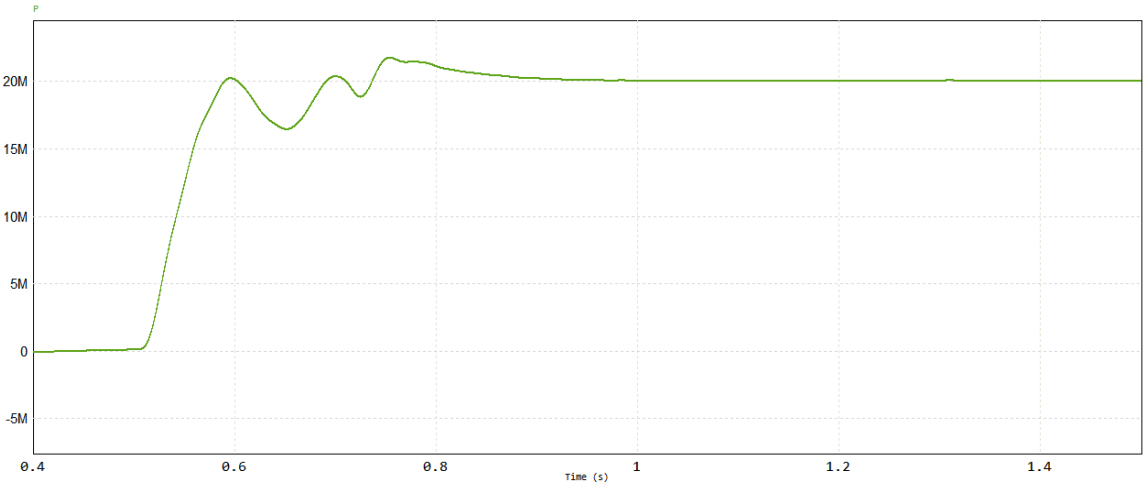

Figure 4.14 - Power supplied in the second test.

Regarding the third test, the initial value of the current was once again 0 A, simulating a situation where 0 MW are fed to the catenary. At the timestamp of 0.5 seconds, the value changes to -476.19 A, representing a situation where 20 MW are being sent from the catenary to the power grid. It is important to mention that this test, just like the second one, is very extreme, as a sudden decrease in power demand from 0 MW to -20 MW is not expected in a real-world situation. This test looks to analyse the behaviour of the conversion module in a situation where trains are regenerating. The power generated by trains when braking is nowhere near as high as the power they consume while in traction mode, so a situation where 20 MW are flowing from the catenary to a substation is unlikely to happen, which contributes even more to the extreme nature of this test.

In Figure 4.15 there is a representation of the voltage in the DC-link for this simulation for a period between 0.4 and 1.5 seconds. Before that, the voltage value stabilizes at around 42 kV at 0.4 seconds, as expected, just like in the previous experiment. At 0.5 seconds, it suffers a big instability caused by the sudden decrease in the current value, making the voltage increase, before stabilizing once again at around 42 kV, at 1.3 seconds. This voltage increase is significant, reaching approximately 53 kV, and can be problematic for the equipment´s health. Under more realistic condition, with lower power level and much smaller gradient, the overvoltage would be very much reduced.

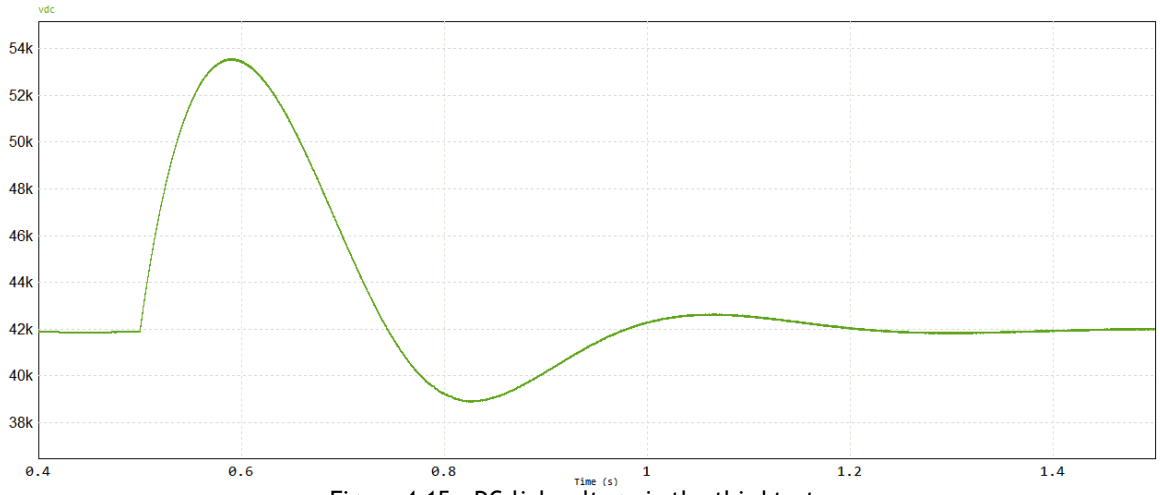

Figure 4.15 – DC-link voltage in the third test

A similar behaviour is seen in the power supplied, represented in Figure 4.16, for the same period of Figure 4.15. At first, there is some instability (not shown), before the value stabilises at around 0 MW, as expected, because there is no load. At 0.5 seconds, it suffers a big instability caused by the sudden increase in the current value, before stabilizing once again at around 20 MW, as expected.

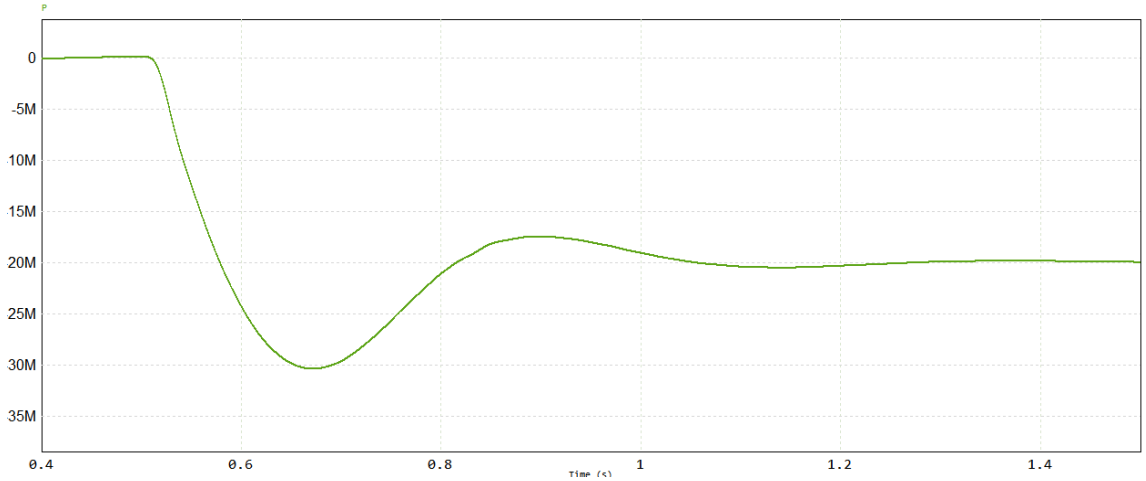

Figure 4.16 - Power supplied in the third test.

Just like in the previous simulation, the currents on the three-phase side are represented between 0.4 and 1.5 seconds, in Figure 4.17.

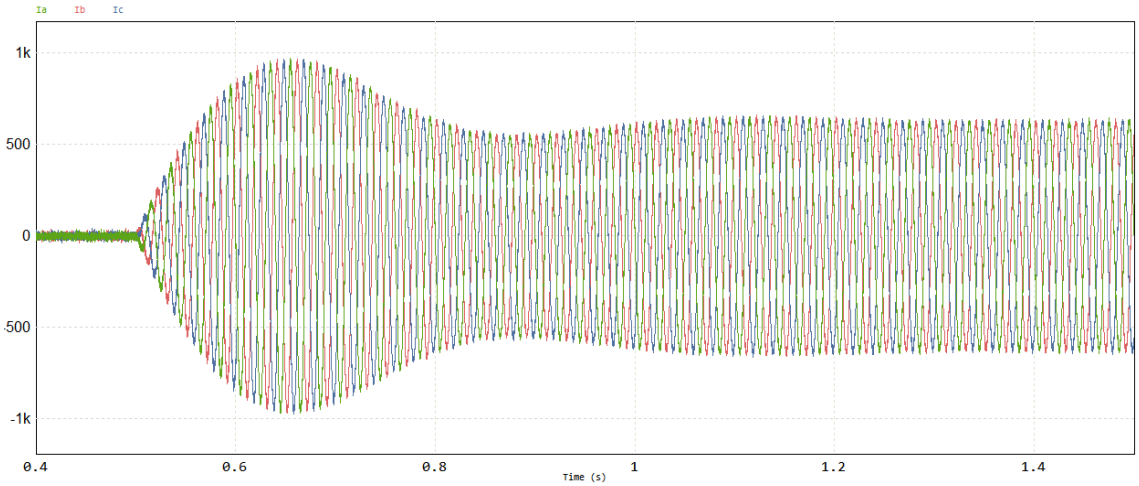

Figure 4.17 - Currents on the three-phase side in the third test.

The results obtained are relatively similar to the ones of the second simulation, with the current values increasing after the current step of the DC-link and stabilizing after a period of instability. The only difference is that this time the current reaches higher peaks during the instability period.

4.3 – Design of the single-phase DC/AC conversion module

The second stage of the project of the traction substation consists of the design of a DC/AC converter. Unlike in the previous converter, this time an MMC topology, based on half-bridge submodules, was selected, after careful consideration, given that this time the converter is single-phase, and the issues regarding controllability and simulation time are reduced. This converter is connected to the DC-link of the AC/DC converter, previously studied, which, for simplification, is represented by a DC source. Considering a maximum peak voltage of 42 kV to be coherent with the previously obtained voltage value of 42 kV for the DC-link, two arms of 28 modules of two transistors were used, 14 up and 14 down. This way is it possible to guarantee a voltage value of around 3 kV per transistor. Given the characteristics of the previously mentioned IGBT FZ1800R45HL4, fabricated by Infineon, it could be used for this MMC model, [18].

An example of some two-transistor submodule can be seen in Figure 4.18. Each module receives two control signals, which are complementary, meaning that while the transistor on top is on, the one on the bottom is off, and vice-versa. The module is connected in parallel with a capacitor. This capacitor is pre-charged to 3 kV, by the 42 kV of the DC link, allowing the transistor that is turned on to have a 3 kV voltage as soon as the simulation starts, [21].

To represent the DC-link, particularly its voltage values, voltage sources were used, totalizing the previously approached 42 kV.

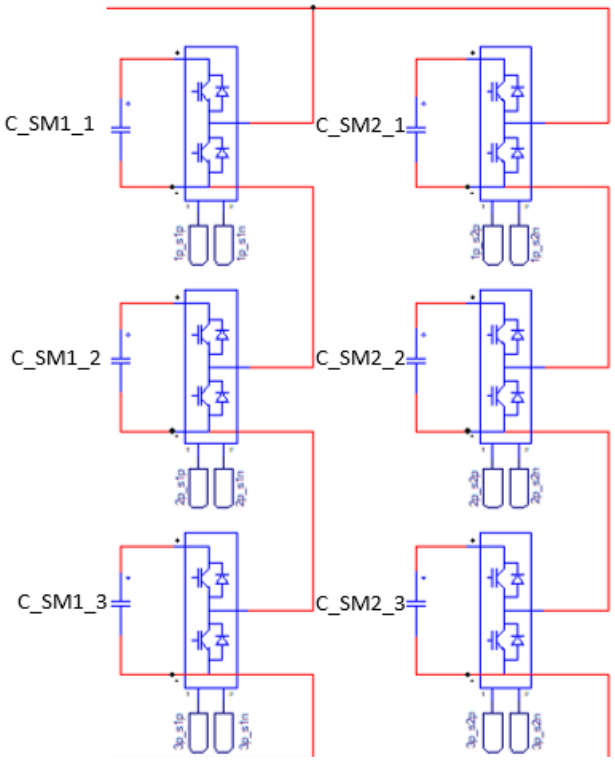

Figure 4.18 - Submodules of two transistors (half-bridge) with a capacitor in parallel.

In the connection between the upper and lower part of both arms two inductances of 5 mH were used to reduce the circulating current. To simplify the model, the control system does not include either circulating current, nor voltage control for the capacitors of the submodules. Plus, an LC filter was designed to place between the inverter and the catenary line, with a 5 mH value for L and a 10 uF value for C. It is a low pass filter with a double pole at 712 Hz, eliminating harmonics and allowing the output voltage to be closer to a perfect sinewave. This can be seen in Figure 4.19.

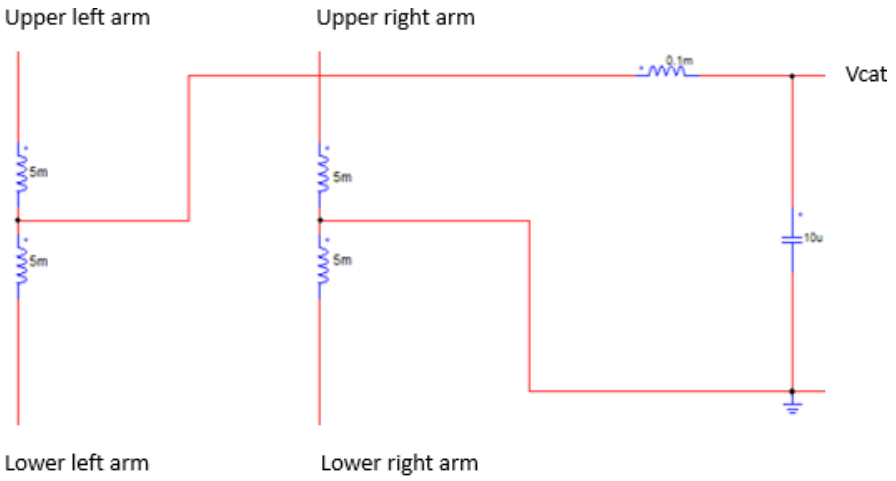

Figure 4.19 - Connection between both ends of each arm and LC filter.

This converter needs to be controlled to deliver the desired voltage on its output end. As previously mentioned, the RMS value of this voltage is 27.5 kV, which matches the highest

permanent limit established in IEC 60850. The instantaneous RMS value of this voltage is permanently measured, and used in generating a control signal, through the process represented in Figure 4.20. This process consists of comparing the present output voltage value with the 27.5 kV reference and obtaining a signal that consists of the difference between both. This error signal is further processed, by a PI controller and multiplying it by a normalized sinewave, a necessity to produce an AC voltage in the connection to the catenary, [5].

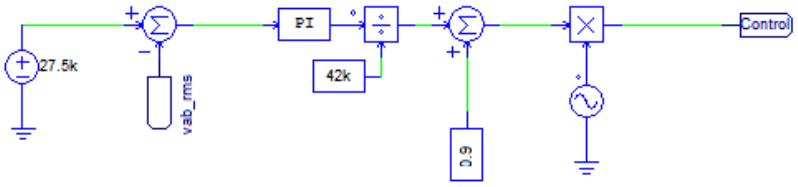

Figure 4.20 - Generation of the control signal.

The previously generated control signal is then processed by multiple PWM blocks, generating the final control signals. For these PWM blocks a switching frequency of 1 kHz was chosen. Each block has a particular phase delay, depending on the component they are controlling, providing the phase shift in the controller. In Figure 4.21 there is the representation of this process for the control of the two modules on top of the upper left arm of the converter. It should be noted that the PWM block can be defined for single our double-edge modulation and includes dead-time. [21].

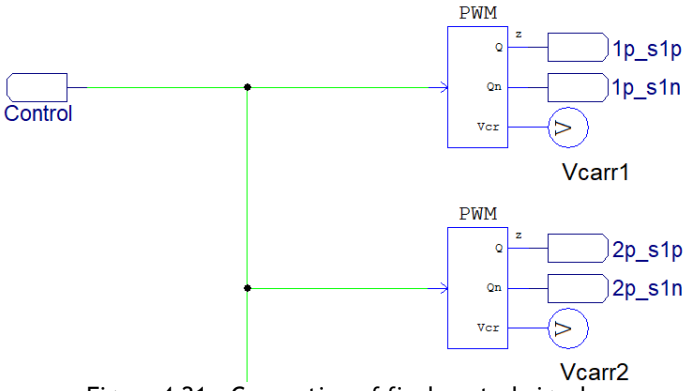

Figure 4.21 - Generation of final control signals.

4.4 – Testing of the single-phase DC/AC conversion module

A series of simulations were planned and executed to better understand the behaviour of different components of the DC/AC conversion module and check if it managed to deliver its overall goal of providing an output voltage with a pre-determined RMS value and react well in transitory situations, where the load characteristics change suddenly.

Four different simulations were done. The first simulation was done in a permanent regime, to check some basic characteristics of the converter, and its ability to deliver a secondary voltage of 27.5 kV. It lasts a total of 1 second. There is a load connected in the

catenary connecting end of the converter, represented by a 100 Ω resistor. With this resistance, there is a power factor of 1, as there is no inductance, and overall power delivery of 7.56 MW, as shown by equation 4.6.

$$P = \frac{V^2}{R} = \frac{27.5k^2}{100} = 7.56\ MW \tag{4.6}$$

Different measurements were done during this test and are presented next. First, it is shown a representation of the output voltage, in Figure 4.22, towards the end of the simulation, more precisely between 0.9 and 0.95 seconds. This representation shows that the converter manages to deliver a voltage that is close to a perfect sinewave, with very little harmonic interference. The THD value is merely 0.0118. This shows that the LC filter design produces good results. For the same period, Figure 4.23 represents the voltage in the upper left arm.

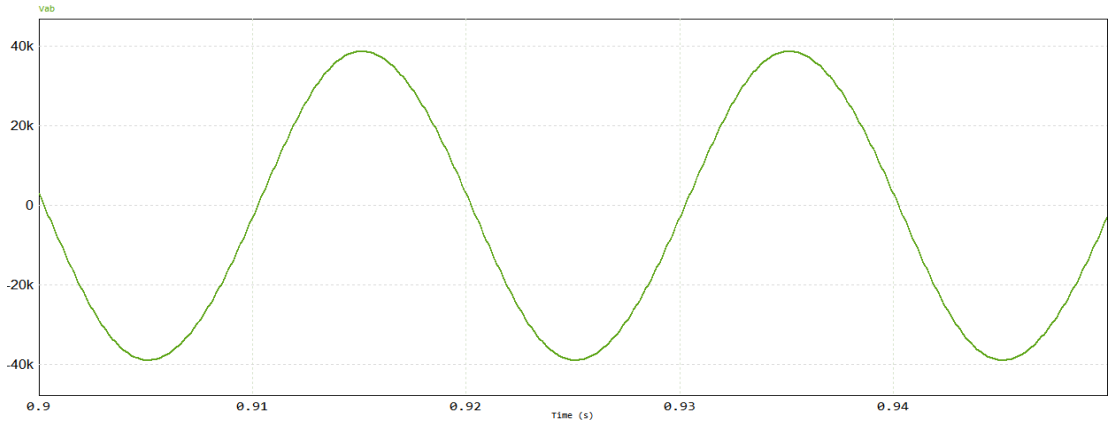

Figure 4.22 - Output voltage in the first simulation.

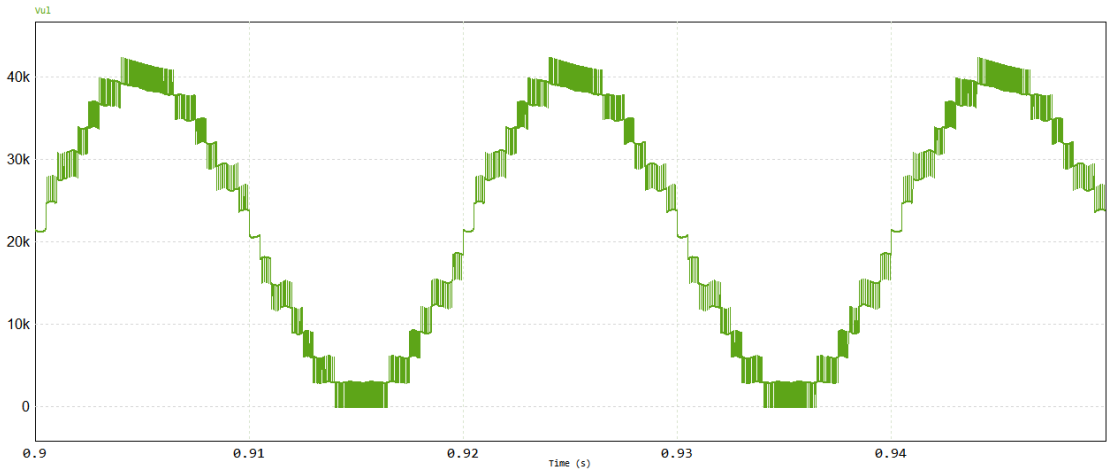

Figure 4.23 - Voltage in the upper left arm in the first simulation.

Analyzing Figure 4.23, it is noticeable that the value of the voltage on the upper left arm varies between 0 V and 42 kV. Given that the converter´s output voltage value results from the difference between the middle points of the left arm and the right arm, a few conclusions can be taken. When the value in Figure 4.23 is at 0 V, the voltage values for the other arms are 42 kV in the lower left arm, 42 kV on the upper right arm and 0 kV on the lower

right arm, meaning that the difference between the two middle points of the arms is 42 kV, as seen in Figure 4.22.

To show the conversion module´s ability to deliver a 27.5 kV voltage in the connection to the catenary, the RMS value of the voltage was also measured, and it is represented in Figure 4.24, throughout the entire simulation.

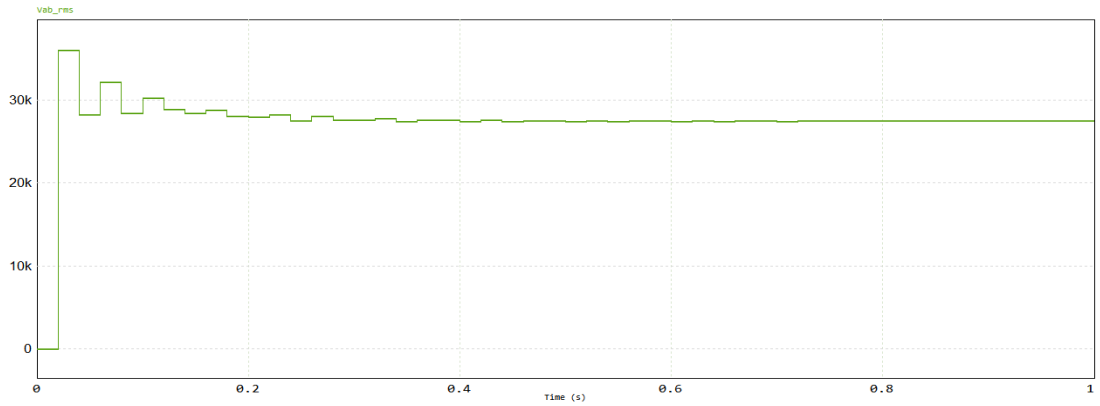

Figure 4.24 - Output voltage (RMS) in the first simulation.

It is noticeable that after a period of higher instability at the beginning of the simulation, the RMS value gradually moves towards its desired final value. At the 0.3 seconds timestamp, it is already around the final value, and at 0.8 seconds it has reached the target, with eventual changes being nonsignificant.

In steady state, the waveform of the current in the load resembles a nearly perfect sinewave, as shown in Figure 4.25, because it is the result of the voltage that is also a nearly perfect sinewave. The only exception is the initial period where there is some instability, which is normal given that the converter is still far from its stable working point.

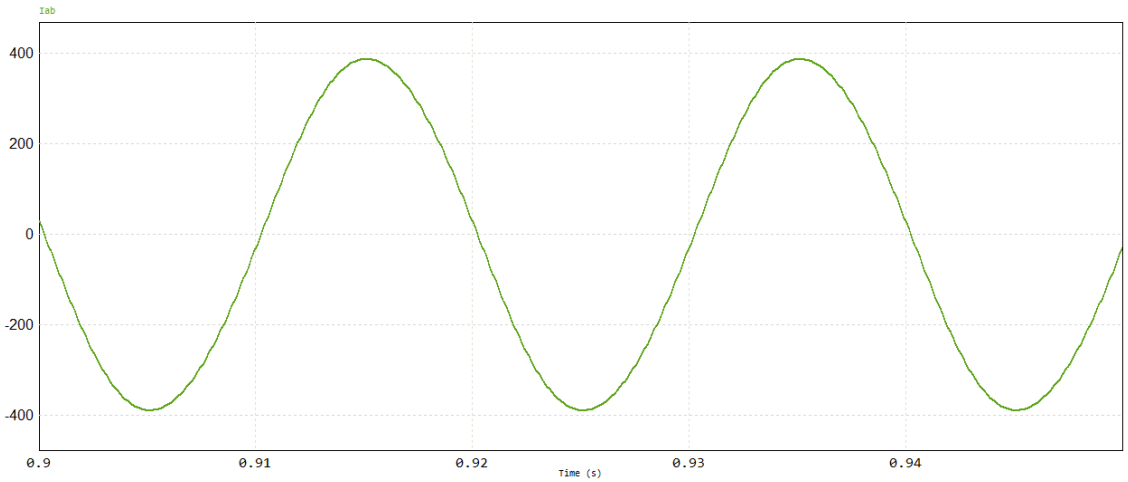

Figure 4.25 - Output current in the first simulation.

For the period between 0.9 and 0.95 seconds, Figure 4.26 shows the representation of the voltages in two capacitors, placed in two submodules of different arms. The fact that they are in different arms, explains the 180º phase shift between them. It is interesting to notice

that both keep their voltage values above 2.9 kV and below 3.1 kV, always. This means that they behave well, being always close to the desired and pre-charged value of 3 kV, and consequently giving to the operating transistor of the module a voltage value close to 3 kV.

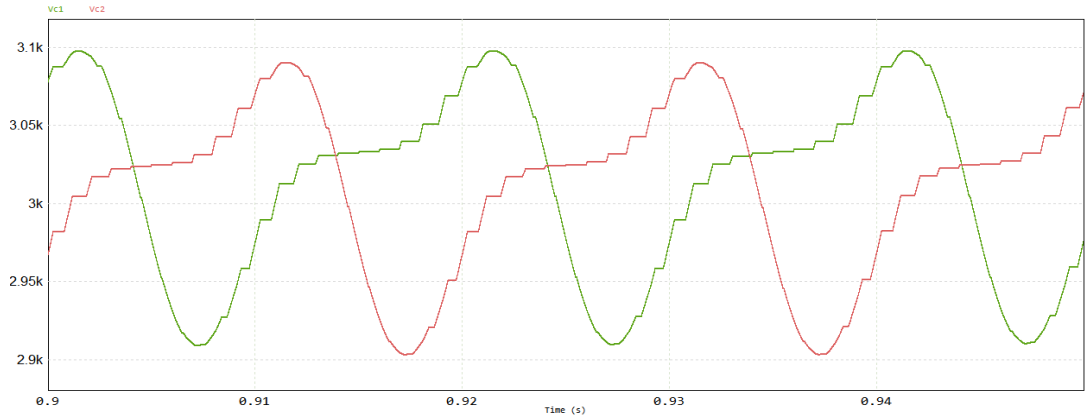

Figure 4.26 - Voltage in two capacitors in different arms.

Figure 4.27 shows a representation of the voltage value of a transistor located in the upper left arm of the MMC converter. Analyzing the results, it is noticeable that the voltage is always either 0 V or close to 3 kV. When this transistor is on, it is 0 V. When this transistor is off, it takes the capacitor´s voltage, which is close to 3 kV, as previously seen.

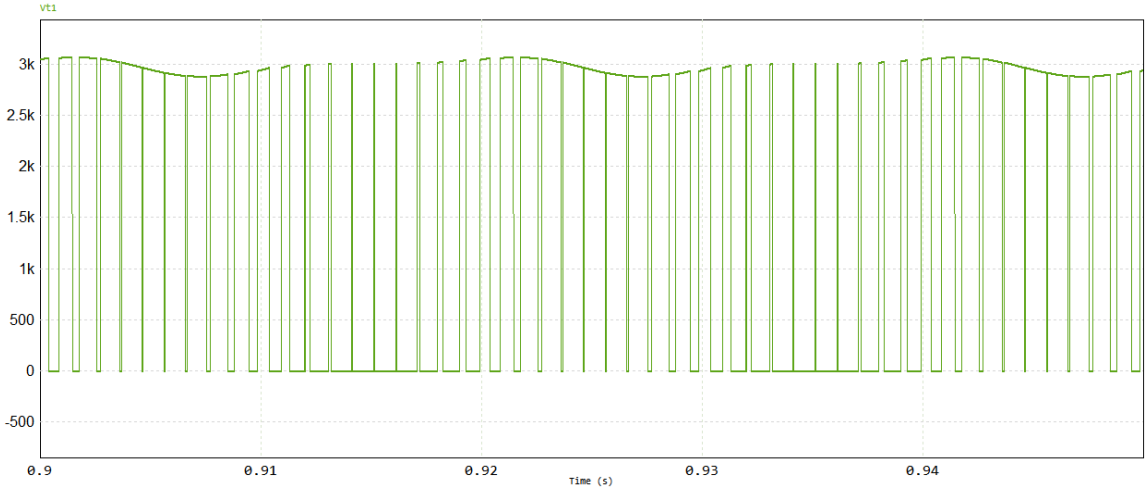

Figure 4.27 - Voltage in the transistor.

To present the previously mentioned phase delay, two different carrier waves were taken and represented in Figure 4.28. These carrier waves are associated with the PWM modules that control the two modules closer to the top of the upper left arm. Both signals are equal triangular waves, with a 1 kHz frequency and are between -1 and 1. The only difference is a slight phase shift, responsible for reducing the THD of the converter output voltage, thus only requiring a relatively small filter.

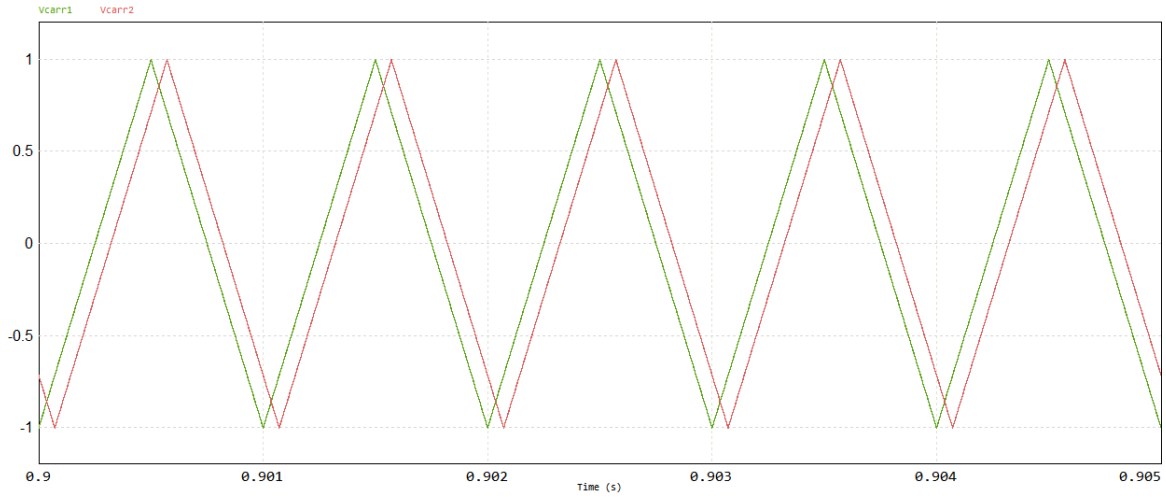

Figure 4.28 - Carrier waves.

The second simulation tests the converter´s ability to respond to a situation where the load increases suddenly. Taking the scenario of the first simulation as a base, with a 100 Ω resistor, this time a new load appears at 0.7 seconds. This load is represented by an AC current source with a peak value of 514 A. This value intends to represent a locomotive consuming 10 MW.

Adding the power consumed by both loads, a total of 17.56 MW is fed by the substation after the 0.7 seconds mark. The total simulation time is 2 seconds.

The representation of the RMS value of the output voltage of the converter is in Figure 4.29, for a period between 0.6 and 1.5 seconds. After the initial period where only the resistor is active as a load, the introduction of the current source results in a small instability. This instability takes the stabilized voltage value and makes it oscillate roughly between 26.7 kV and 28.5 kV, during an initial period. This oscillation gets progressively smaller and gets nearly insignificant after 1.1 seconds of simulation. It gets fully stabilized near 1.3 seconds.

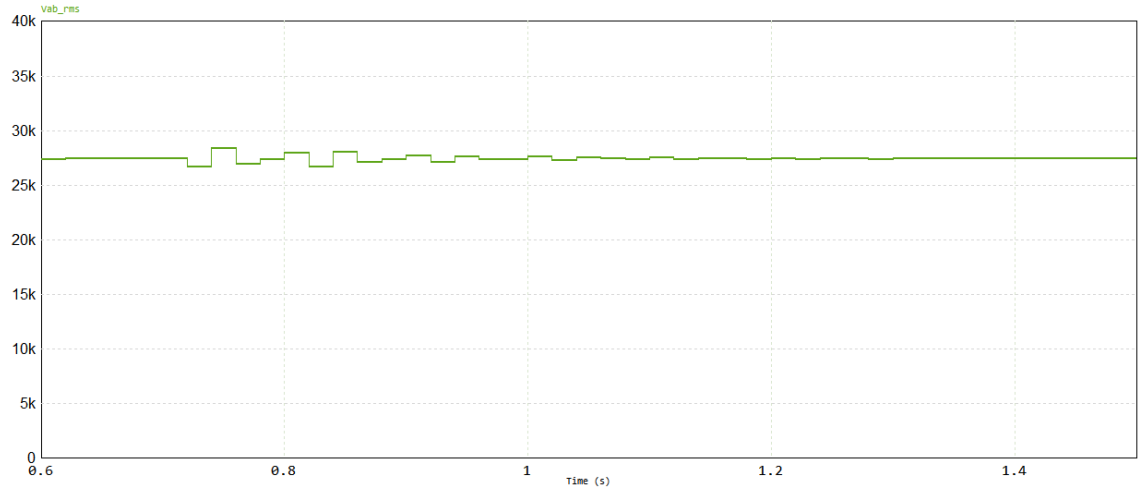

Figure 4.29 - Output voltage (RMS) in the second simulation.

In Figure 4.30 there is the representation of the catenary current for the same period, between 0.6 and 1.5 seconds. This period shows the appearance of the new load at 0.7 seconds, and as a result there is big increase in the current values. Given that the new load has a unitary

power factor and is consuming, the phase of the current wave remains the same after its appearance.

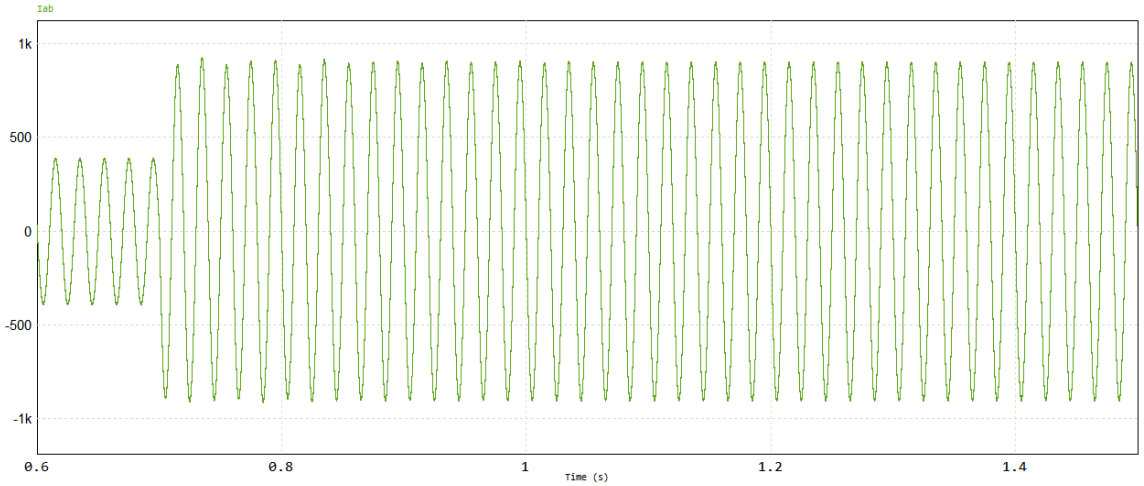

Figure 4.30 - Current in the catenary in the second simulation.

Figure 4.31 shows the output voltage waveform, again between 0.6 and 1.5 seconds.

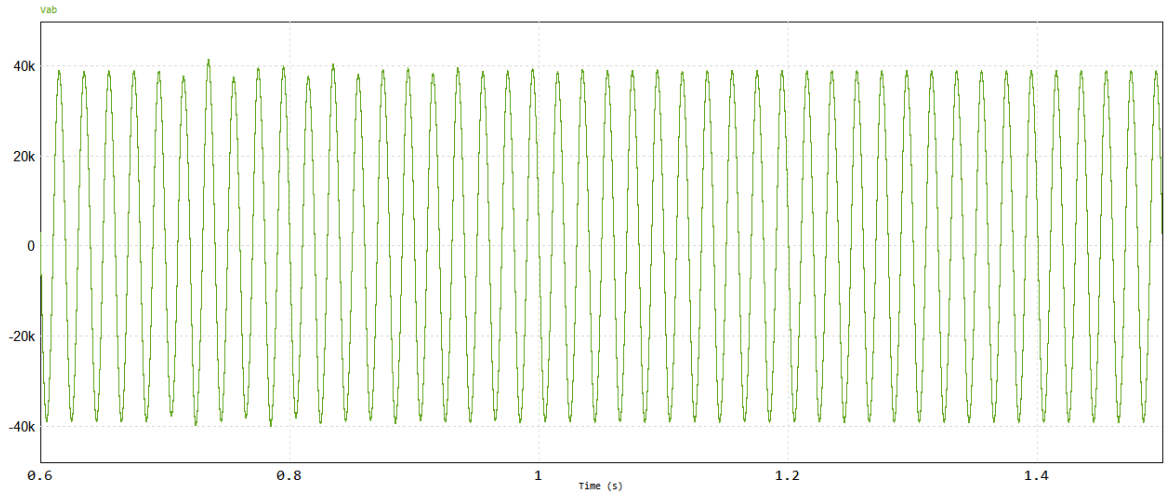

Figure 4.32 - Output voltage in the transitory period of the second simulation.

The period represented in Figure 4.31 includes the moment when the current source load appears at 0.7 seconds. While the sine´s periods are apparently equal between each other up until 0.7 seconds, after that, they visibly lose their uniformity because of the instability, with some periods reaching higher peak voltage values, while others reaching lower peak values. This instability gets progressively less significant trough time.

The current in the DC end of the converter is represented in Figure 4.32, in the period between 0.6 and 1.5 seconds. After a period of satisfactory stability, the appearance of a new load at 0.7 seconds creates an instable scenario. Since the new load condition demands more current, the DC current values are also higher. This instability gets progressively smaller with time as the converter gets closer to finding its new working point.

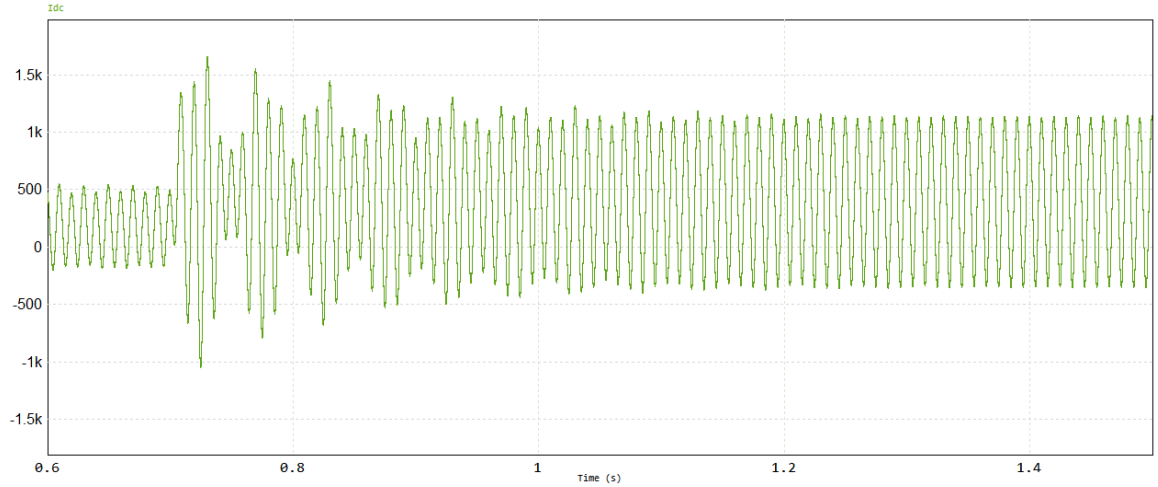

Figure 4.32 - Current in the DC end of the second simulation.

The third simulation tests the converter´s ability to respond to a sudden drop in power demand, getting to a point where the power is flowing from locomotives to the substation. Taking the initial scenario of the first and second simulations, with only the resistor operating, this time a new load, represented again by an AC current source, appears at 0.7 seconds, injecting current in the catenary. The peak value of this current is 771 A, which was calculated for a 15 MW power regeneration value. This is a quite exaggerated regenerative power, used here for pushing the converter´s limits.

Combining this value with the power consumed by the resistor, the overall power flowing from the catenary to the substation is 7.44 MW, after 0.7 seconds. The simulation has a total of 2 seconds.

Figure 4.33 shows the RMS value of the output voltage, in a period between 0.6 and 1.5 seconds.

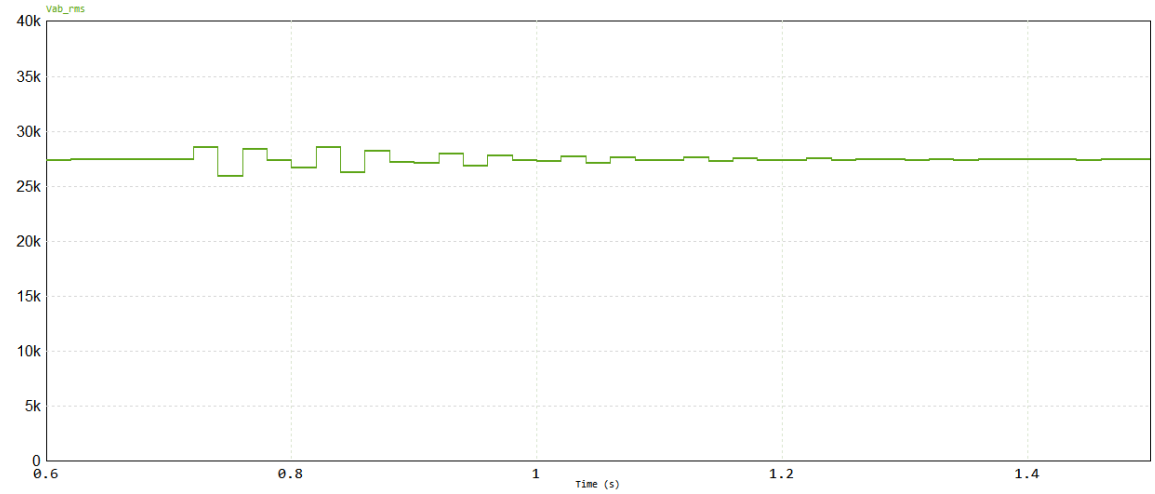

Figure 4.33 - Output voltage (RMS) in the third simulation.

The result presented in Figure 4.33 is similar to the one obtained in the second simulation, with the instability caused by the AC current source making the already stabilized voltage oscillate between 26 and 28.5 kV. Just like in the previous simulation, the oscillations

lose force with time, and get near the stabilization level around 1.2 seconds and fully stabilized around 1.5 seconds. The fact that this time the difference in load introduced by the appearance of the AC current source is bigger than in the second experiment explains why the catenary´s RMS voltage value takes longer to stabilize. Other than that, no significant differences can be seen when comparing the simulations between them and the moments when the substation is feeding energy to the catenary with the moments it is receiving energy. This is a positive, as it shows that the converter remains relatively stable regardless of the power flow scenario.

The current in the catenary is represented in Figure 4.34 for a period between 0.6 and 1.5 seconds. As previously mentioned, the appearance of a new load changes the power situation from a consumption of 7.56 MW to a regeneration of 7.44 MW. These two values are very similar and consequently no big difference is seen in the peak current values before and after the appearance of the new load. However, there is a clear change of 180º in the phase that comes with the transition from consuming to regenerating.

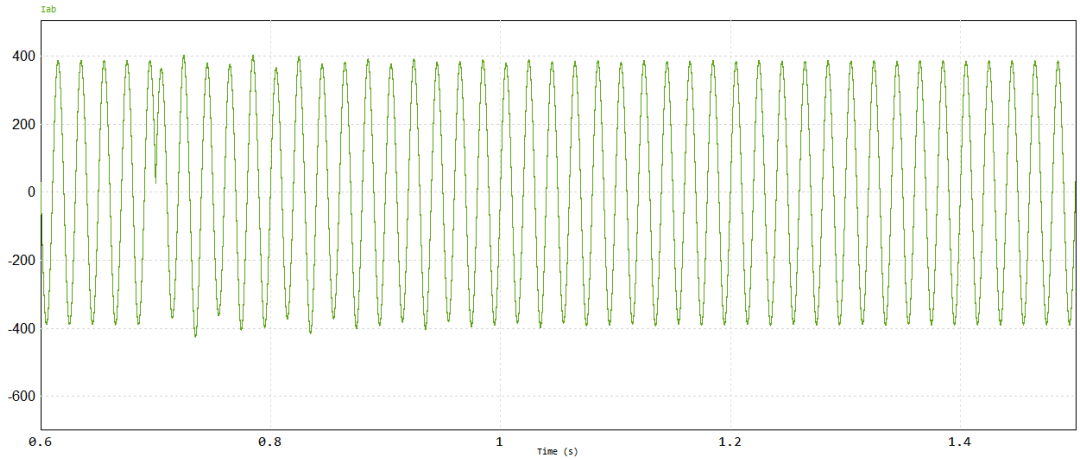

Figure 4.34 - Current in the catenary in the second simulation.

Finally, the current in the DC end is also presented, in Figure 4.35. This time, the instability is slightly bigger when compared to the second simulation, and it takes longer to stabilize as a result.

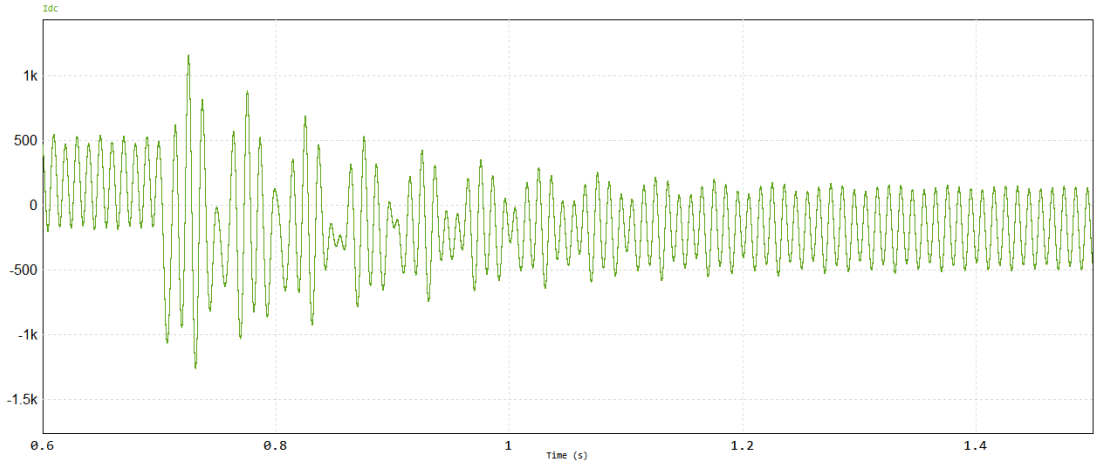

Figure 4.35 - Current in the DC end of the third simulation.

A fourth simulation was done to test the converter´s ability to deal with non-linear loads, lasting a total of 1 second. The results for the output voltage and the catenary current, between 0.94 and 1 second, are represented in Figure 4.36 and Figure 4.37, respectively.

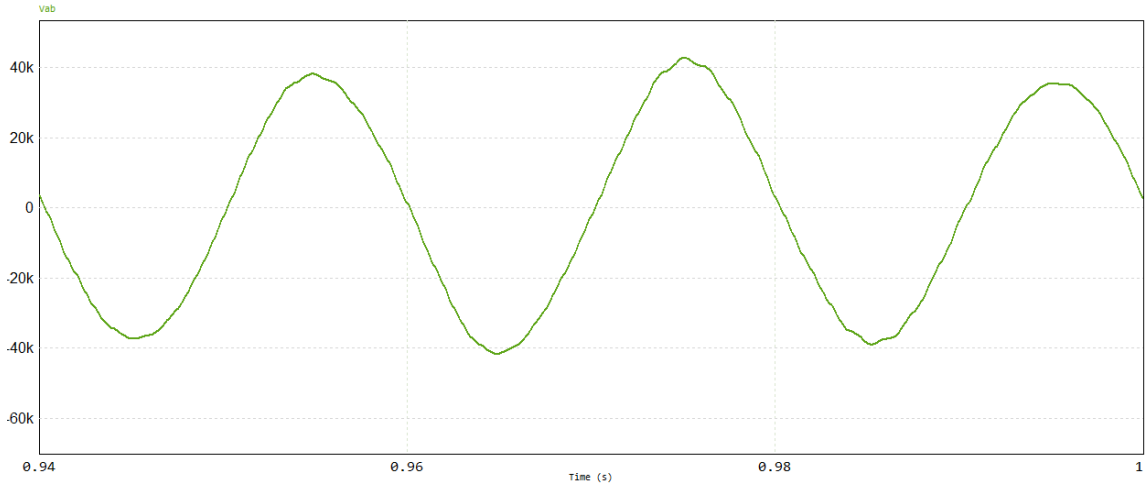

Figure 4.36 – Output voltage in the fourth simulation.

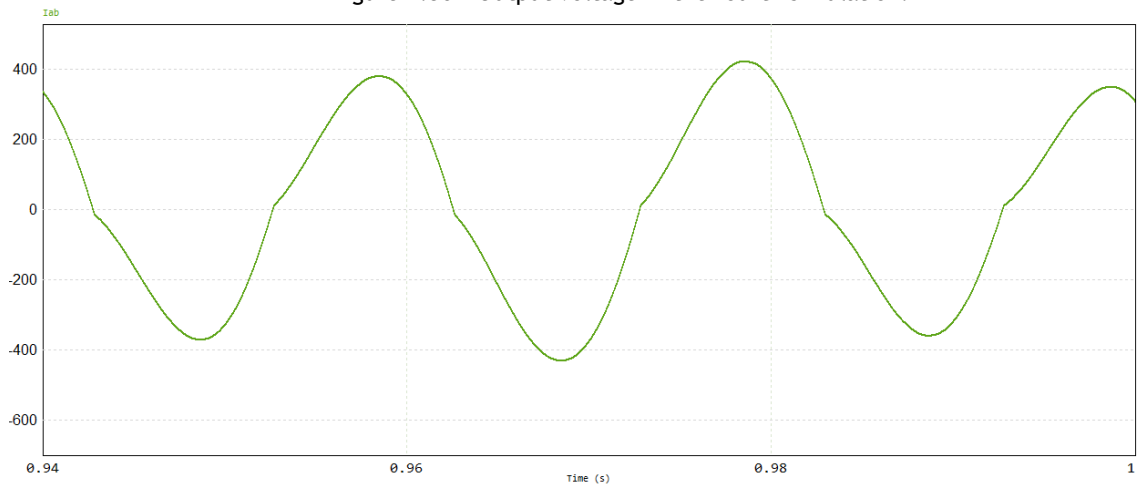

Figure 4.37 – Output current in the fourth simulation.

The non-linear load was built using an inductor, followed by a diode bridge, followed by a resistor and capacitor in parallel. The results represented in Figure 4.35 show that the non-linear load has an impact on the sinewave of the output voltage. The THD value is 0.0346, which is higher than in the previous simulations. Nevertheless, this result is still relatively good as the voltage is still close to a perfect sinewave, which leads to the conclusion that the converter behaves well when working with non-linear loads. Of course, if the load/train current becomes more distorted the same will happen with the voltage.

4.5 – Conclusions

Some of the results obtained, particularly in the second and third tests of the grid connecting converter could potentially be somewhat problematic, given some big overshoots in the DC-link voltage value, during the transitory moments. However, as previously mentioned,

these tests were very extreme. In a less extreme scenario, where the current step is less aggressive and not as sudden, the behaviour of the converter would be more satisfactory. Nevertheless, some work could be done around the controller of the converter, to optimize it and reduce the impact of the instabilities during the transitory periods, both regarding the overshoots magnitude and the time it takes to stabilize.

Overall, it can be concluded that the grid connecting converter operates in a way that respects International and European standards and manages to stabilize the voltage value of the DC-link at 42 kV, responding satisfactorily well to the sudden changes in the power demand.

Looking at the results obtained in the simulations of the catenary connecting converter, it is possible to conclude that it manages to establish the desired voltage in the catenary connection and responds reasonably well to sudden instabilities regarding the loads. However, while the simulations do not show a case like that, other than throughout the initial instability associated with the initiation of the converter´s operation, more aggressive current steps could lead to over voltages that exceed the maximum non-permanent value of 29 kV for the catenary voltage established by IEC 60850, which is an issue, [5].

Further development of the catenary connecting converter could be done, regarding the controller, to speed up the stabilization process and make sure that the changes in load condition do not result in any standards being disrespected. Nevertheless, the response to the challenges presented is already satisfactory.

Chapter 5

Control and simulation of two substations in parallel

Having already developed a fully functional model for a substation, capable of converting the power from an external source into power that can be injected into the catenary with a controllable voltage module and phase, it is now important to study how two substations can operate in parallel. Regarding this topic, it is particularly important to understand how the controllability of the substations can be used to regulate the active power flow in the catenary. The substations must work in a coordinated manner, recuring to local measurements, and remote ones also. The control strategy is responsible for defining the parameters of each substation, [22].

To speed-up the simulation process, an average model was used for each substation. This model consists of a DC voltage source and a controlled current source on one side, and a controlled voltage source followed by a filter, connecting to the catenary. The use of a constant DC voltage source is because it is fast and accurately controlled by the converter connecting the substation to the power grid as demonstrated in Chapter 4. Similarly, since the study in this chapter relates to power flow control at fundamental frequency only, the use of an average model for the inverter is justified. The goal of the control system is to produce a control signal that results in a certain voltage magnitude and phase in the catenary, considering a final goal. An example of this substation model is represented in Figure 5.1.

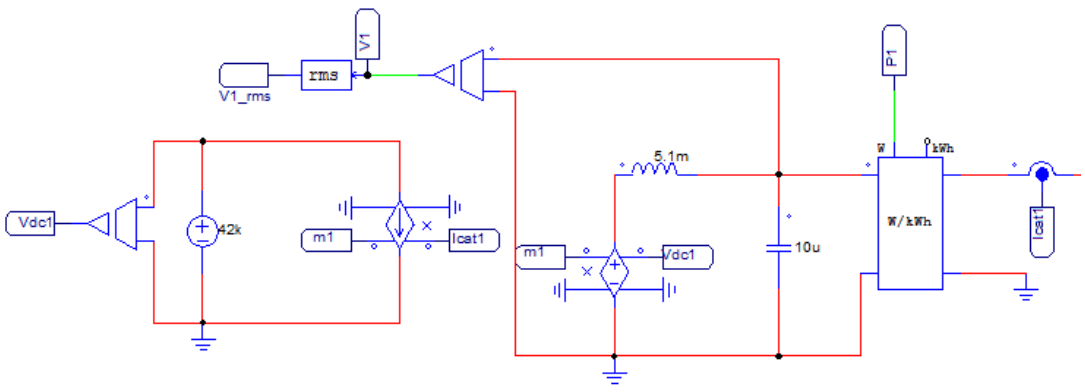

Figure 5.1 - Average model of a substation.

Looking at Figure 5.1, it is noticeable that many measurements are being made. The most important measurements are the V1_rms which represents the RMS value of the voltage at the point connecting the substation to the catenary, which is being used in the substation control system, and the P1 value which represents the active power being supplied by substation 1, which is being used in the overall model control system. It is also noticeable the presence of a 5.1 mH inductance and a 10 uF capacitor. These represent the filter at the exit of the substation that makes the catenary voltage sinewave be as perfect as possible in the point connecting the substation and the catenary.

For the simulations present in this chapter, two substations were placed on opposite ends of a 50 km catenary. Regarding this catenary, it is represented by a line divided into six sections. These consist of two 5 km sections, one immediately next to each of the substations, and four 10 km sections, between the two 5 km sections. In a simulation environment, the locomotives can be placed between any two adjacent sections, as well as between a substation and its adjacent section, giving them a total of 7 potential positions, as shown in Figure 5.2, where the blue dots represent the positions, and the distance value of the axis represents the distance from that position to the first substation. For example, if a locomotive is in Position 1 it is passing by the first substation and if it is in Position 3 it is located 15 km from the first substation and 35 km from the second one. As previously mentioned, the typical values used for the catenary resistance and inductance are 0.1 Ω/km and 1 mH/km, respectively. As referred before, for power flow studies the capacitance can be neglected.

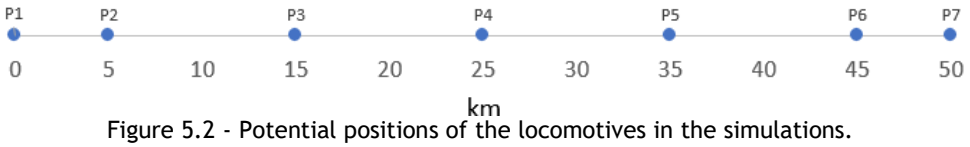

Figure 5.2 - Potential positions of the locomotives in the simulations.

5.1 – Development of a control system for the overall model

The main goal of controlling the overall model is to manipulate the way active power flows from the substations to the locomotives. There are different methods for achieving this. Some examples include grid-feeding, which consists in picking or calculating certain reference values for the active and reactive power and using them in the controller, so that it can make the necessary changes to the substations´ parameters, to make it feed the desired power, grid-forming which consists in maintaining stable voltage and frequency values in the substation and grid-supporting, which consists in making the substations share the loads in proportion to their power capacity, [22][23]. For the first substation, the control´s goal is simply to establish a reference voltage, as this is simply a reference substation with a voltage output that is constant in both magnitude and phase. A simple control circuit was developed and is represented in Figure 5.3.

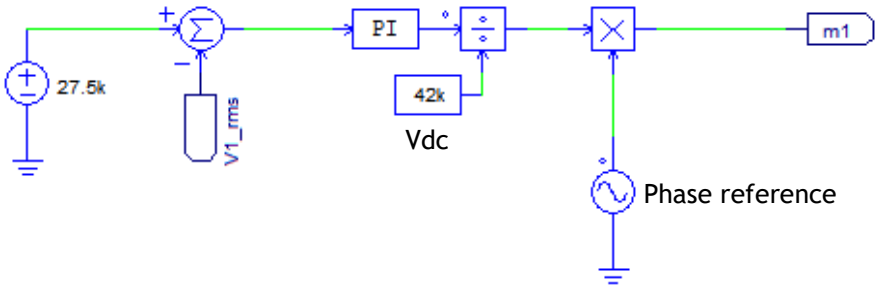

Figure 5.3 - Control circuit of the first substation.

In this control circuit, the RMS value of the catenary voltage at the substation is subtracted from the reference magnitude for the voltage, which is 27.5 kV. The resulting value is then processed by a PI controller and multiplied by a normalized sinewave with a phase angle considered 0, which serves as a reference. The generated signal is then used to control the voltage source responsible for the voltage value at the point where the substation meets the catenary.

Regarding the second substation, the control circuit must be more complex, because the first substation acts merely as a reference. To better understand the process behind it, it is important to look at Equation 5.1, which represents the active power flow in a line where the reactance is significantly superior to the resistance. V1 and V2 are the RMS values of the voltage in each substation, X=ωL and δ is the phase difference between the two voltages, [24].

$$P = \frac{V1 * V2 * \sin \delta}{X} \tag{5.1}$$

Equation 5.1 shows that, in this case, the active power flow can be easily controlled by manipulating the voltage phase angle´s difference between the two sources.

Therefore, it is of greater utility to develop a control system capable of altering the voltage´s phase angle of the second substation and keeping its magnitude at 27.5 kV, taking the parameters of the first one as a reference, to obtain the desired power flow goals.

It is also important to establish a criterion for the power flow goals. In this system, a relatively simple and initial criterion of making both substations feed the same active power value to the catenary was chosen. In a more complex case that emulates a real-life scenario, where more substations are used and data such as the locations of the locomotives could be known to the control system, it would be possible to develop more advanced controllers, capable of managing the power flow considering more interesting goals, like reduction of power losses in the catenary, which would translate in financial benefits for the operators.

Taking the previously mentioned criteria, it is necessary to produce a reference value for the power injected by the second substation in the catenary. This is generated by adding the total active power injected by the first and second substations in the catenary and dividing it by two. This way, the reference value is half of the total active power injected in the catenary, as desired. After this process, the actual active power being fed by the second substation is subtracted from the reference value, generating a signal that is the difference between the two. This signal goes through a PI controller to generate a delta for the phase

angle of the voltage in the second substation. The circuits responsible for generating this delta are represented in Figure 5.4.

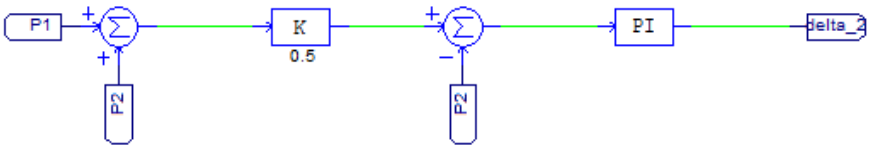

Figure 5.4 - Generation of the delta value for the second substation´s voltage phase angle.

This delta value is then used to generate a sinewave responsible for controlling the phase angle of the voltage in the second substation. To give the system an initial point to work from, a subsystem based on switches was developed so that for the first 0.2 seconds of each simulation the voltage phase angle of the first substation is the same as the second substation. After that, the manipulated signal is introduced. This signal is generated by producing the sine of the addition between the present phase angle of the second substation and the previously mentioned delta value. The circuits responsible for making the described operation are represented in Figure 5.5.

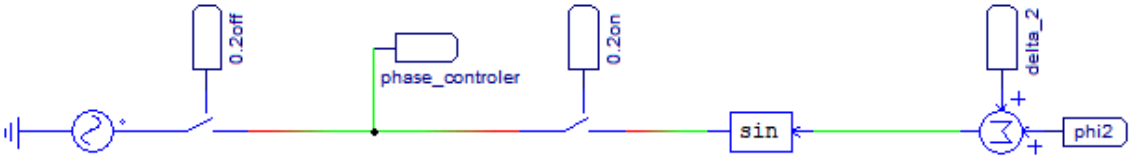

Figure 5.5 - Generation of the signal responsible for controlling the phase angle of the second substation´s voltage phase angle.

After that, the resulting phase control signal is used in the second substation´s controller. This follows the same process as the first substation and can be seen in Figure 5.6.

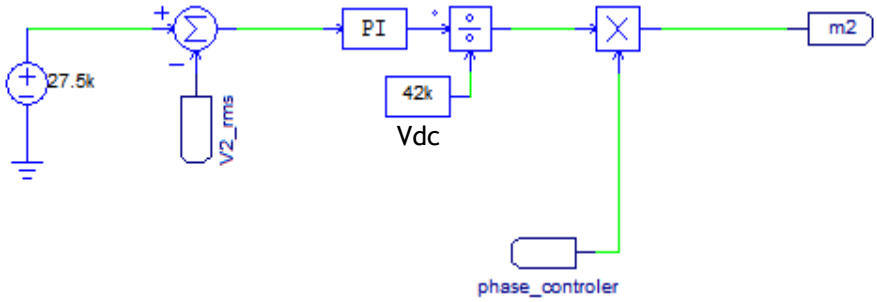

Figure 5.6 - Control circuit of the second substation.

5.2 - Simulation of the two substations in parallel mode

For these simulations, current sources were used to represent the locomotives. Regarding the current value and phase angle for each locomotive´s representation, these were picked to obtain a certain power considering a 27.5 kV voltage magnitude and a certain power factor, considering that the voltage phase is the same as the first substation. As a result, given

the voltage drops or increases in the catenary, the active power consumed by each locomotive will be slightly different than it was projected, and given the current flowing in the catenary, the power factor will also be slightly different than it was projected for, most of the time. To test the developed model and show the potential of the control of the substation´s voltages, some simulations were performed under two different scenarios.

5.2.1 – Open-loop control in the first scenario

The first scenario is a simple one, where no more than one locomotive is operating at the catenary at any given time and pretends to show the basic capabilities of the model. More precisely, a total span of four seconds was simulated. From the timestamp of 0 seconds to 1 second a locomotive, named Locomotive 1, is operating in position 3 with a projected power of 8 MW and an inductive power factor of about 0.91. From 1 second to 2 seconds a locomotive, named Locomotive 2, is operating in position 5 with a projected power of 6 MW and an inductive power factor of about 0.88. From 2 seconds to 3 seconds a locomotive, named Locomotive 3 is operating in position 2 and is braking and regenerating power, injecting into the catenary a projected power of 3 MW, and with an inductive power factor of about 0.94. From 3 to 4 seconds a locomotive, named Locomotive 4, is operating in position 6 with a projected power of 10 MW and an inductive power factor of about 0.93. The graphic of Figure 5.7 shows the relative position of each locomotive.

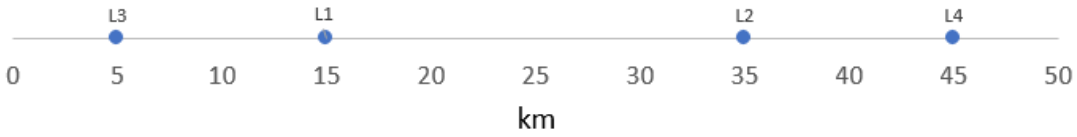

Figure 5.7 - Relative position of the locomotives in the first scenario.

The graphics of Figures 5.8, 5.9, 5.10, and 5.11 shows the working timeline of each locomotive, with green meaning that it is consuming, red meaning that it is regenerating and grey meaning that it is not in contact with the catenary.

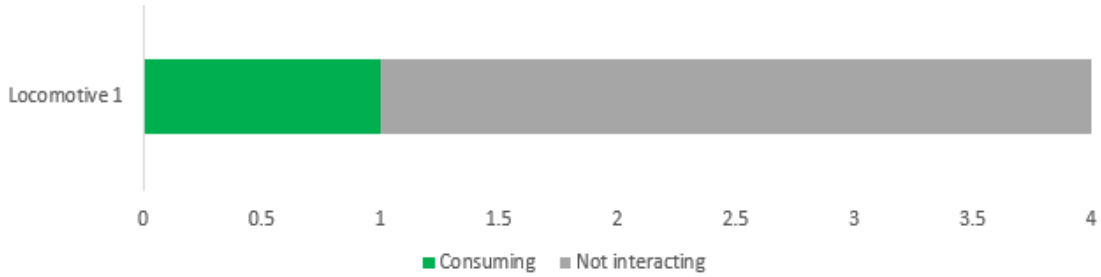

Figure 5.8 - Working timeline of Locomotive 1 in the first scenario.

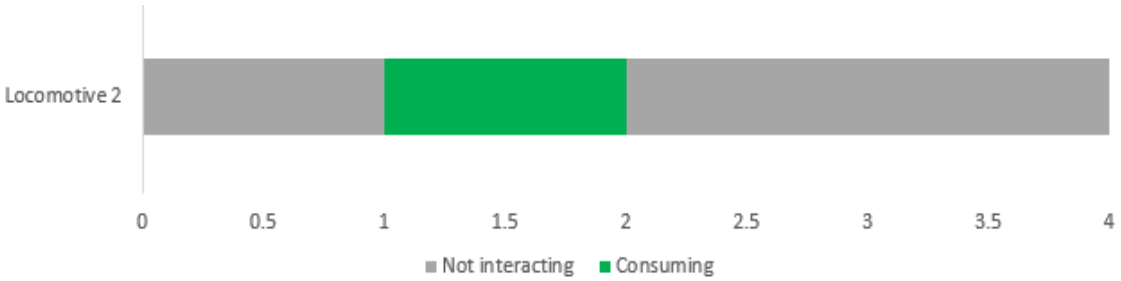

Figure 5.9 - Working timeline of Locomotive 2 in the first scenario.

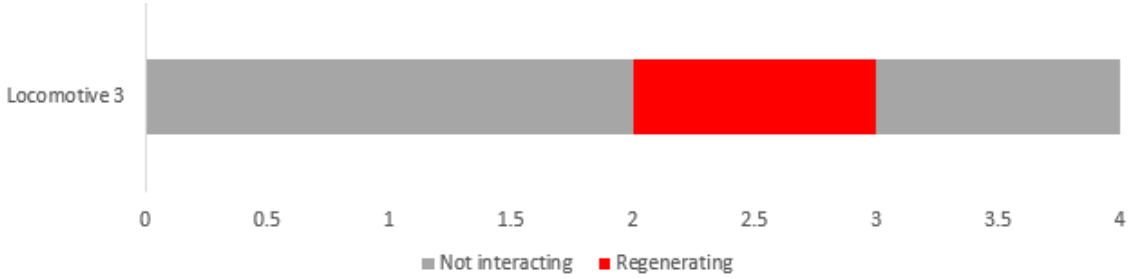

Figure 5.10 - Working timeline of Locomotive 3 in the first scenario.

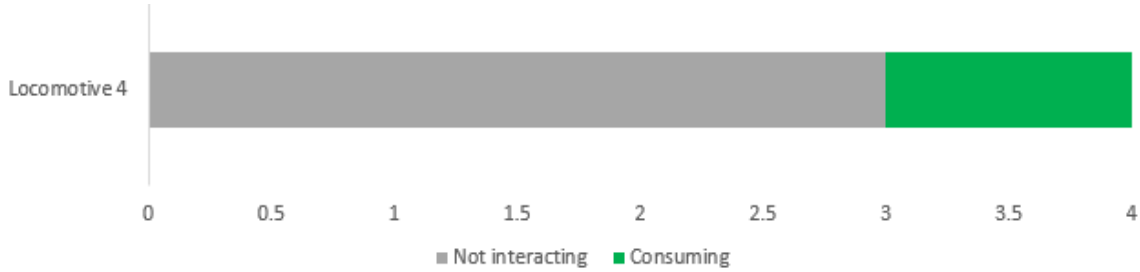

Figure 5.11 - Working timeline of Locomotive 4 in the first scenario.

To show the impact of the control system, two different simulations were performed under this scenario. The first one was done with no overall control system, keeping both substations´ voltages at 27.5 kV magnitude and the same phase angle.

Considering the active power injected into the catenary by each substation, it is possible to see four different periods, as shown in Figure 5.12. During the first second, after a transitory time of about 0.3 seconds, the power injected by the first substation stabilizes at around 5.5 MW and the power injected by the second substation at around 1.85 MW. At the 1-second timestamp, there is an instability caused by Locomotive 1 leaving the line and Locomotive 2 entering the line. After that, the power injected by the first substation stabilizes at around 2.15 MW, and the power injected by the second substation at around 3.15 MW. At the 2 seconds timestamp, there is an instability caused by Locomotive 2 leaving the line and Locomotive 3 entering the line. After that, the power injected by the first substation stabilizes at around -2.56 MW, and the power injected by the second substation at around -250 kW. In this segment, the values are negative because Locomotive 3 is regenerating. At the 3-second timestamp, there is an instability caused by Locomotive 3 leaving the line and Locomotive 4 entering the line. After that, the power injected by the first substation stabilizes at around 2.2 MW, and the power injected by the second substation at around 7.15 MW. It is important to mention that, since there is no overall control system operating, these results come from

simple power flow calculations, and the power needed by each locomotive tends to flow in higher quantities from the nearest substation, and lower quantities from the substation that is further away. As an example, Locomotive 1 (between 0 seconds and 1 second) is in Position 3, closer to the first substation and getting more power from it, while Locomotive 4 (between 3 seconds and 4 seconds) is in Position 6, closer to the second substation and getting more power from it.

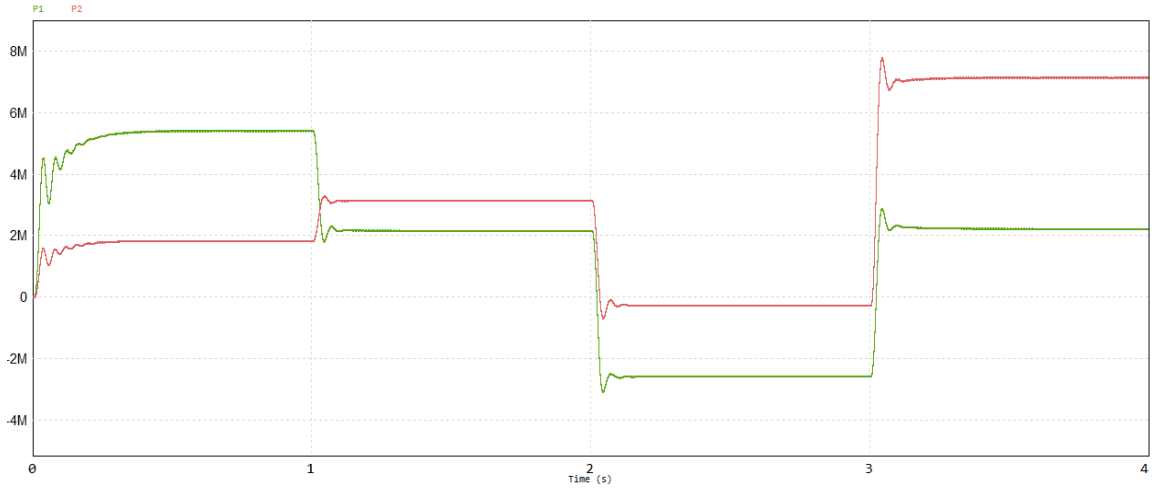

Figure 5.12 - Total power injected into the catenary by each substation in the first simulation of the first scenario.

The losses are also an important aspect of this system. In Table 5.1 they are represented for each period. Although difficult to compare given the different nature and position of the locomotives, it is apparent that these are higher for higher power cases. This occurs because higher powers mean higher currents going through the catenary, which combined with the catenary´s impedance results in higher losses. They are also very dependent on the power factor. When Locomotive 1 is operating the losses are higher than when Locomotive 4 is operating, despite the higher power needs of Locomotive 4. This fact can be explained in part by the higher inductive power factor of Locomotive 4, in comparison to the one from Locomotive 1.

Table 5.1 - Power losses in the first simulation of the first scenario

Period	Losses (kW)
0s – 1s	89
1s – 2s	52.5
2s – 3s	5.3
3s – 4s	71.9

Finally, the catenary voltages are also interesting to look at, to study their variation. In Table 5.2 the values of the RMS voltage in Position 3, 15 km from the first substation and 35 km from the second one, are represented. Taking a closer look, it is possible to see that for the first, second, and fourth periods, the voltage value drops concerning the 27.5 kV from the substations. This happens because of the impedance of the catenary combined with the current flowing from the substations to the locomotive. Nevertheless, these values are still well within the permanent values allowed in IEC 60850, so they are not an issue. On the other hand, the

voltage value in the third period is above 27.5 kV. This happens because in this period, the only locomotive in the catenary is regenerating and the current is flowing from the locomotive to the substations. This value is above the highest permanent value previewed in IEC 60850 but below the highest non-permanent value of 29 kV. Following the parameters of the mentioned international standard, this overvoltage should not last more than five minutes in a real-world situation, [5].

Table 5.2 - Voltage in Position 3 in the second simulation of the first scenario.

Period	Voltage in Position 3 (kV)
0s – 1s	26.83
1s – 2s	27.27
2s – 3s	27.58
3s – 4s	27.38

5.2.2 – Active power control in the first scenario

Taking into consideration the same scenario, another simulation was performed, this time with the overall control system in operation. In Figure 5.13 there is the representation of the power supplied by each substation. Analyzing it and comparing it with the results of the previous simulation, the difference is that this time the values of the power supplied by each substation converge to the same value, as expected, because of the impact of the control. After each transitory moment, where locomotives stop or start operating in this catenary, the power values diverge but then start converging again until reaching the same value. In the first period, the power supplied by each substation converges to 3.615 MW, in the second period the power supplied by each substation converges to 2.675 MW, in the third period the power supplied by each substation converges to -1.405 MW and in the fourth period the power supplied by each substation converges to 4.83 MW.

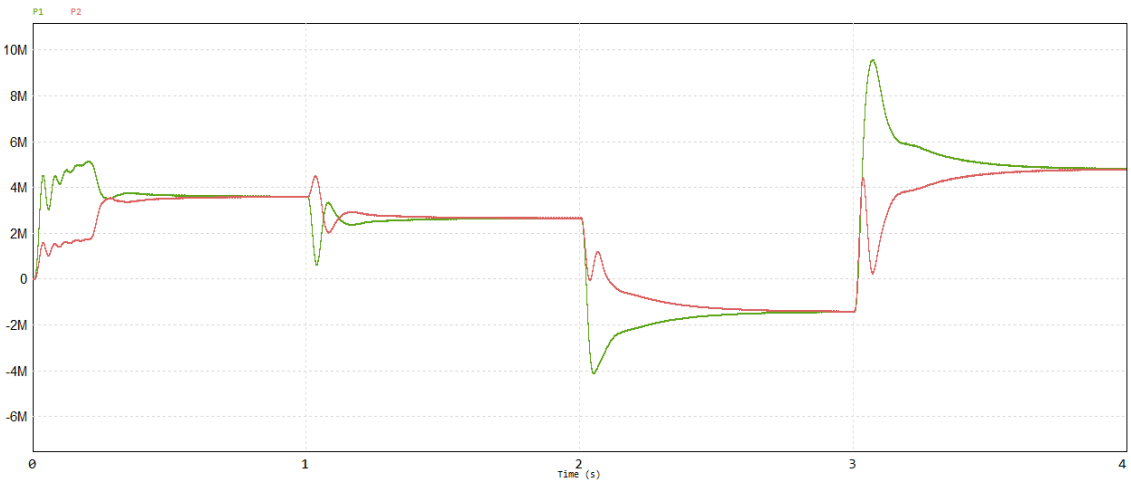

Figure 5.13 - Total power injected into the catenary by each substation in the second simulation of the first scenario.

In Table 5.3 the losses for each period are represented. Comparing them to the ones obtained in the previous simulation, they are significantly higher. Given the way the controller

was set up, this is an expected result. The substations are forced to feed the same amount of power to the catenary, which leads to higher currents having to cross longer sections of the catenary, in most cases. As a result, the losses are higher.

Table 5.3 - Power losses in the second simulation of the first scenario.

Period	Losses (kW)
0s – 1s	104
1s – 2s	58
2s – 3s	14
3s – 4s	168

In Table 5.4 the RMS voltage in Position 3 is represented for each period. In comparison to the ones obtained in the previous simulation, the values are equal, which leads to the conclusion that the changes in the current and power flow imposed by the controller had little or no impact on the catenary voltages. The issue associated with the voltage in the third period being above the highest permanent limit established by IEC 60850 remains and must disappear within five minutes in a real-world situation, [5].

Table 5.4 - Voltage in Position 3 in the second simulation of the first scenario.

Period	Voltage in Position 3 (kV)
0s – 1s	26.83
1s – 2s	27.27
2s – 3s	27.58
3s – 4s	27.38

5.2.3 – Open-loop control in the second scenario

The second scenario is more complex and involves situations where more than one locomotive is operating in the catenary simultaneously. When the simulation starts there is a locomotive with a projected power of 6 MW in position 4, with an inductive power factor near 0.935, named Locomotive 1. There is also a locomotive with a 7 MW projected power in position 6, with an inductive power factor near 0.89, named Locomotive 2. At the 1.8 timestamp, Locomotive 1 starts braking and regenerating a projected power of 2 MW. At the 3.2 seconds timestamp a new locomotive with a projected power of 8 MW starts operating in position 2, with an inductive power factor of nearly 0.84, named Locomotive 3. At the 4.2 seconds timestamp Locomotive 1 stops operating. A new locomotive with a projected power of 10 MW shows up at position 3, with an inductive power factor of nearly 0.91, named Locomotive 4, at the 5.4 seconds timestamp. Locomotive 2 stops operating at the 5.6 seconds timestamp. At the 6.6 seconds timestamp, Locomotive 4 starts braking and regenerating a projected power of 3 MW and at the 7.6 timestamp Locomotive 3 stops operating. Once again two simulations were done, one with no overall control system, where the voltage magnitude and phase angle of both substations are the same, and one with the overall control system active. Just like in the

previous scenario, the graphic of Figure 5.14 shows the relative position of each locomotive, following the same format.

Figure 5.14 - Relative position of the locomotives in the second scenario.

The graphics of Figures 5.15, 5.16, 5.17 and 5.18 shows their working timeline, once again following the green, red, and grey colour scheme, like in the first scenario.

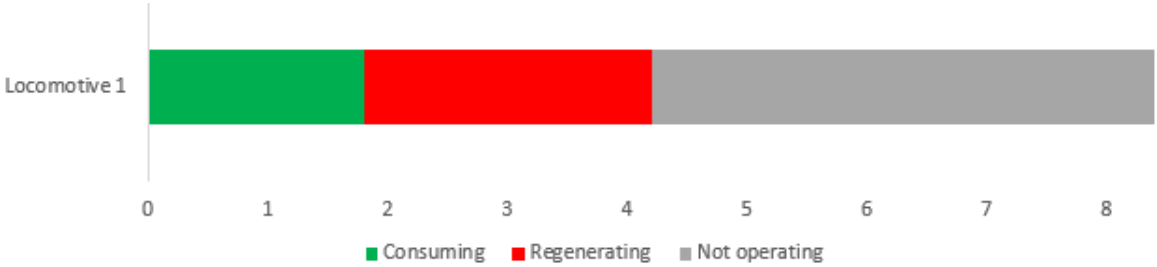

Figure 5.15 - Working timeline of Locomotive 1 in the second scenario.

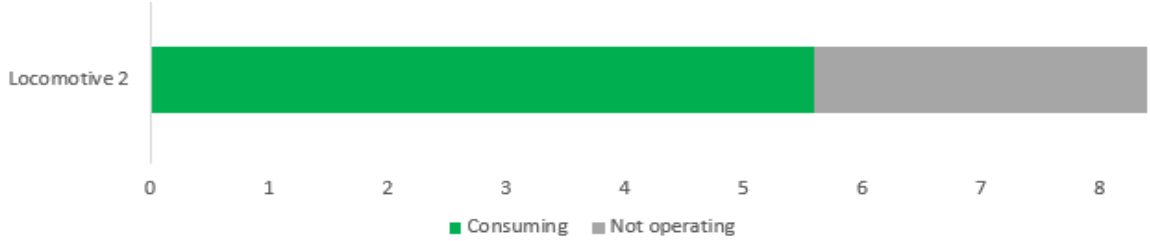

Figure 5.16 - Working timeline of Locomotive 2 in the second scenario.

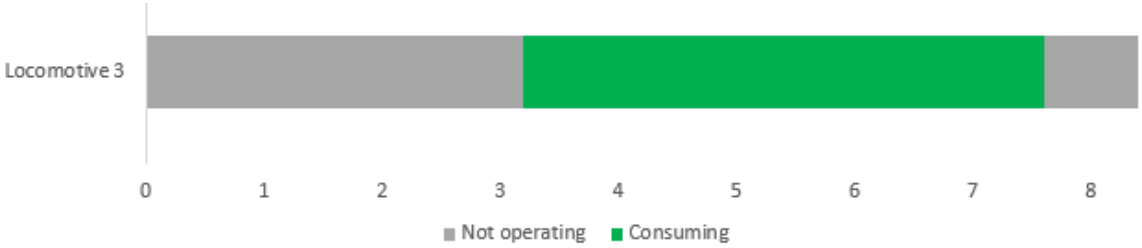

Figure 5.17 - Working timeline of Locomotive 3 in the second scenario.

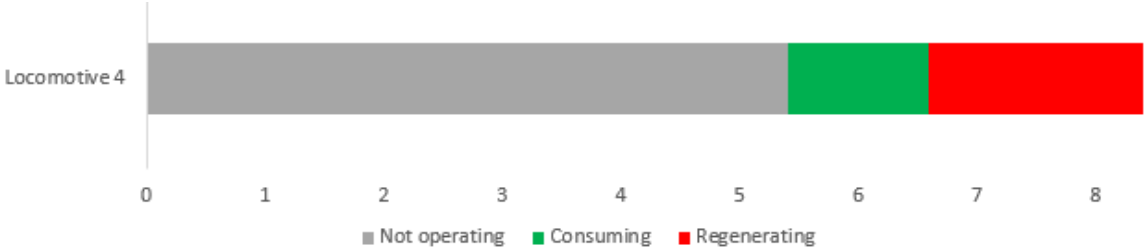

Figure 5.18 - Working timeline of Locomotive 4 in the second scenario.

In Figure 5.18 there is the representation of the power flow in the first simulation of this scenario, its 8 distinct periods.

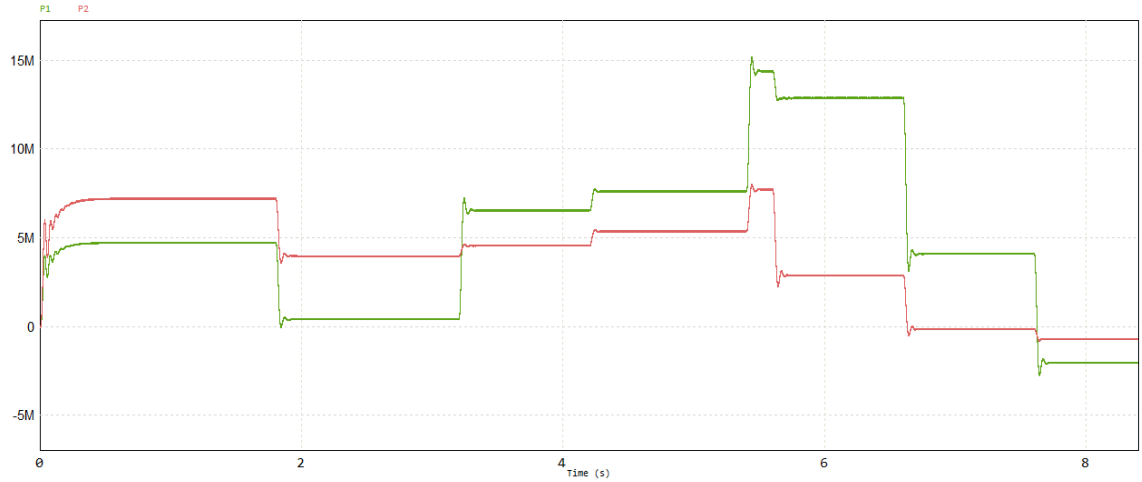

Figure 5.19 - Total power injected into the catenary by each substation in the first simulation of the second scenario.

Just like in the first simulation of the previous scenario, the nonexistence of an overall control system makes the active power flow in higher quantities from the substation that is closer to the locomotive. Depending on which locomotives are active in the catenary and their parameters, there are periods of higher power flow like between 5.6 seconds and 6.6 seconds, and lower power flow like between 1.8 seconds and 3.2 seconds. The period between 6.6 seconds and 7.6 seconds is particularly interesting, because the first substation is injecting power, and the second one is almost not supplying power. This happens because Locomotive 3 is consuming close to the first substation, while Locomotive 4 is regenerating close to the middle of the catenary resulting in this interesting scenario. The only period of this simulation where both substations are receiving power is the last one, between 7.6 seconds and 8.4 seconds, where the only locomotive operating in the catenary is regenerating.

The loss analysis is also an important one. Table 5.5 represents the losses for each period. As expected, the total losses are particularly higher when the power values are higher, such as between 5.4 and 5.6 seconds and between 5.6 and 6.6 seconds. Given the fact that multiple locomotives operate at the same time in this scenario, it is difficult to analyze the impact of the power factor of each one on the periods. Nevertheless, it remains important to have high power factors to minimize losses.

Table 5.5 - Power losses in the first simulation of the second scenario.

Period	Losses (kW)
0s – 1.8s	128.5
1.8s – 3.2s	30.5
3.2s – 4.2s	66.5
4.2s – 5.4s	81.5
5.4s - 5.6s	328
5.6s - 6.6s	252
6.6s - 7.6s	28.5
7.6s - 8.4s	12.5

Just like in the previous scenario, the RMS voltage values in position 3, 15 km from the first substation and 35 km from the second one, were taken for each period, and are

represented in Table 9. Analysing the values, it is noticeable that for most periods, these are below the 27.5 kV of the substations, because of the current flow from the substation to the locomotives and the catenary´s impedance. The higher the power flow, the lower the voltage values. Just like in the previous scenario, situations, where locomotives are regenerating, tend to create over voltages. Although every period between 1.8 and 4.2 seconds and between 6.6 and 8.4 seconds has a locomotive regenerating, for most of this time the presence of locomotives consuming compensates the current injected into the catenary by the locomotives in regenerating process. The only exception is between 7.6 and 8.4 seconds, where only Locomotive 4 is operating, and is regenerating. In this period, the voltage in position 3 is above the highest permanent limit displayed in IEC 60850, a situation that cannot last over 5 minutes. For the period between 5.4 and 5.6 seconds, the voltage in Position 3 does not stabilize, because this is a very short period, so it was kept out of Table 5.6, [5].

Table 5.6 - Voltage in Position 3 in the first simulation of the second scenario.

Period	Voltage in Position 3 (kV)
0s – 1.8s	26.92
1.8s – 3.2s	27.5
3.2s – 4.2s	26.94
4.2s – 5.4s	27.15
5.4s – 5.6s	-
5.6s - 6.6s	26.42
6.6s - 7.6s	27.49
7.6s - 8.4s	27.76

5.2.4 – Active power control in the second scenario

The analysis made of the second simulation follows the same format as the first one, being divided in power flow, losses and voltage drop in the catenary.

In Figure 5.20 there is the representation of the power injected by each substation in the catenary. Much like in the second simulation of the first scenario, after the instability caused by the change in the locomotives´ operating conditions that initiate each period, the power injected by each substation converges to the same value, thanks to the impact of the overall control system. It is interesting to have a look at the period between 5.4 and 5.6 seconds. In this period, the injected power values do not reach the convergence point desired before the next instability-inducing event happens. This occurs because this is a very short period in comparison with the others, and the next instability comes straight away. As a conclusion, the controller needs a few tenths of a second to make the injected powers fully converge to the same value, depending on the instability dimension. For this period, the time before the following instability was not enough for the converter to achieve its target.

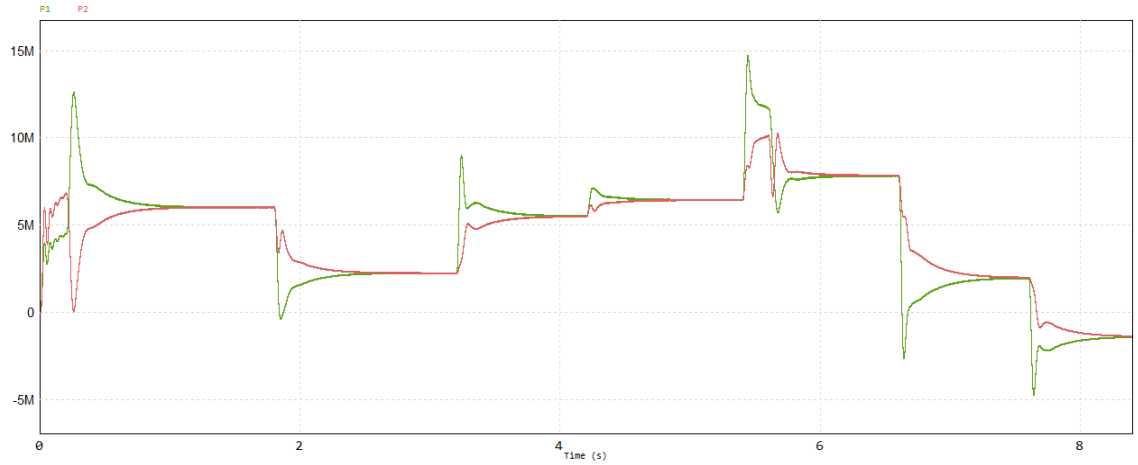

Figure 5.20 - Total power injected into the catenary by each substation in the second simulation of the second scenario.

The losses in the catenary can be seen in Table 5.7. Comparing these values with the ones of the previous simulation, the conclusion is that they are higher for every single period, just like in the first scenario, because the controller changes the natural power flow and forces the active power to go through longer sections of catenary to get to its destination, increasing the losses.

Table 5.7 - Power losses in the second simulation of the second scenario.

Period	Losses (kW)
0s – 1.8s	166
1.8s – 3.2s	74.5
3.2s – 4.2s	62
4.2s – 5.4s	75
5.4s – 5.6s	326
5.6s - 6.6s	405
6.6s - 7.6s	62.5
7.6s - 8.4s	14.4

When it comes to the RMS voltage values in Position 3, these are equal to the ones in the previous simulation, which leads to the conclusion that the controller´s impact is not significant enough to alter this value. Once again, it is important to reinforce that the voltage value in the period between 7.6 and 8.4 seconds must drop below 27.5 kV in less than five minutes in a real-world situation. Once again, it is important to point out that the voltage in the period between 5.4 and 5.6 seconds does not stabilize, so it was kept out of Table 5.8. [5].

Table 5.8 - Voltage in Position 3 in the second simulation of the second scenario.

Period	Voltage in Position 3 (kV)
0s – 1.8s	26.92
1.8s – 3.2s	27.50
3.2s – 4.2s	26.94
4.2s – 5.4s	27.15
5.4s - 5.6s	-
5.6s - 6.6s	26.42
6.6s - 7.6s	27.49
7.6s - 8.4s	27.76

5.3 - Conclusions

The simulations present in this chapter lead to the conclusion that careful control of substations parameters and, consequently, the power flow is an area that can be of great benefit in the future of electrified railways. It also shows that depending on the scenario, some situations may lead to catenary voltage values that are not supported by IEC 60850, but this was due only because the substation voltage set point was set at 27.5 kV. A lower set-point avoids this issue. Regarding the power factor of the locomotives, these simulations show the importance of keeping them as high as possible, because this reduces losses. Given that this is merely a simulation process, the locomotives´ power factors used were not in accordance with EN 50388, which states that all trains consuming over 2 MW must have an inductive power factor above 0.95, [5][10].

The parallel feeding of two or more substations can fulfill other objectives than the one studied in this chapter, namely the management of reactive power at substation level through voltage magnitude control.

Chapter 6

Conclusions and future work

This chapter provides the main conclusions obtained throughout this dissertation project and proposals for future work.

6.1 - Conclusions

Throughout this dissertation project it was seen that the way locomotives are supplied with power has evolved massively, and the technologies associated with this process are vast, and present different advantages and disadvantages. Taking their characteristics and cost and combining that with the characteristics of the railway, such as traffic and the characteristics of the locomotives used is an important part of projecting railways. Power electronics based solutions for getting power from a source to the railways are still an understudied area, although it has great potential.

Throughout this work, the design of a power conversion system, capable of extracting power from an electrical power grid and delivering it to the catenary with a voltage regulated in magnitude and phase has shown that there is great potential to be explored in this solution. The NPC based converter managed to extract power from the AC grid and transform it into DC power at 42 kV, while introducing a relatively low harmonic component and being seen by the grid as balanced load. However, there were still some issues related with the overshoot of the voltage value in the DC-link, when faced with a sudden load change. This overshoot can be dangerous for the equipment. It is also important to point out again that the NPC converter developed could not be used in a real world situation without transformers, because of the limitations associated with the voltage calibre of the transistors.

The MMC based converter managed to transform the DC power from the DC-link into single-phase AC power to be delivered to the catenary at 27.5 kV and in a close to perfect sinewave, with very little harmonic component. However, the time it takes to reach the 27.5 kV target after an instability is not ideal. Overall, it can be concluded that the substation developed reaches its main goal in a satisfactory way, which is delivering the power from the

power grid to the catenary, while achieving the desired voltage values for the DC-link and the catenary connection, but some improvements could be made regarding its reaction to sudden instabilities.

Furthermore, the possibility of using this controllability and combining it with information such as the locations of the locomotives and the operating conditions of other substations is particularly interesting to obtain benefits regarding the power flow, such as power loss reduction. The simulations and analyses represented in this document, although some of them relatively simple, have confirmed the advantages that this type of solution has over the more conventional ones, and show the potential there is for further developments. Considering this, is it now important to study and develop more efficient conversion systems and controllers, so that the integration of power electronics in railway substations can become more of a reality all over the world. It is also important to explore cheaper ways of doing this introduction, as the equipment required tends to be significantly more expensive when compared to the more conventional solutions.

6.2 – Future work

For the future work, it would be interesting to develop an MMC model of the grid connecting converter, so that the overall substation becomes more realistic, and more compatible. In addition, more detailed attention could be paid to the parameters of the controllers, to try to find better working scenarios regarding the overshoots and time it takes the converters to stabilize.

The same can be said about the controller of the two substations working in parallel. This can be improved so that it reaches more interesting goals, such as loss reduction.

References

[1] I. Krastev, P. Tricoli, S. Hillmansen and M. Chen, "Future of Electric Railways: Advanced Electrification Systems with Static Converters for ac Railways," in *IEEE Electrification Magazine*, vol. 4, no. 3, pp. 6-14, Sept. 2016, doi: 10.1109/MELE.2016.2584998.

[2] M. Ceraolo, "Long duration simulations of railway AC Electrified lines," *2018 AEIT International Annual Conference*, Bari, Italy, 2018, pp. 1-6, doi: 10.23919/AEIT.2018.8577344.

[3] Shi-Lin Chen, R.-J. Li, and Pao-Hsiang Hsi, "Traction system unbalance problem-analysis methodologies," in *IEEE Transactions on Power Delivery*, vol. 19, no. 4, pp. 1877-1883, Oct. 2004, doi: 10.1109/TPWRD.2004.829920.

[4] EN 50160 ed. 2 – "Voltage characteristics of electricity supplied by public distribution networks", English version 2007.

[5] IEC 60850: Railway applications – Supply voltages of traction systems, Edition 4.0, 2014.

[6] IEC, "Electromagnetic Compatibility (EMC) - Limits - Assessment of Emission Limits for the Connection of Unbalanced Installations to MV, HV and EHV Power Systems", Technical Report IEC/TR 61000-3-13, Ed. 1, 2008.

[7] P. Paranavithana, U. Jayatunga, S. Perera and P. Ciufo, "A review of recent investigations with reference to IEC/TR 61000-3-13 on voltage unbalance emission allocation," *Proceedings of 14th International Conference on Harmonics and Quality of Power - ICHQP* 2010, 2010, pp. 1-8, doi: 10.1109/ICHQP.2010.5625471.

[8] S. M. Halpin, "Comparison of IEEE and IEC harmonic standards," *IEEE Power Engineering Society General Meeting, 2005*, 2005, pp. 2214-2216 Vol. 3, doi: 10.1109/PES.2005.1489688.

[9] IEC/TR 61000-3-6: Electromagnetic compatibility (EMC) – Part 3-6: Limits – Assessment of emission limits for the connection of distorting installations to MV, HV and EHV power systems, Edition 2.0, 2008.

[10] IEC, EN 50388 – "Railway Applications - Power supply and rolling stock - Technical criteria for the coordination between the power supply (substation) and rolling stock to achieve interoperability", March 2012.

[11] C. Bin-Kwie and G. Bing-Song, "Three phase models of specially connected transformers," in *IEEE Transactions on Power Delivery*, vol. 11, no. 1, pp. 323-330, Jan. 1996, doi: 10.1109/61.484031].

[12] K. Ramadhan, K. Yonathan, I. M. Ardita, F. H. Jufri and A. R. Utomo, "Voltage Stability Improvement Using Load Shedding and Static VAR Compensator (SVC): Study Case of Senayan-Sambas Power System," *2019 IEEE International Conference on Innovative Research and Development (ICIRD)*, Jakarta, Indonesia, 2019, pp. 1-5, doi: 10.1109/ICIRD47319.2019.9074752.

[13]W. Qiong, J. Qirong and W. Yingdong, "Study on Railway Unified Power Quality Controller based on STATCOM technology," *2011 5th International Power Engineering and Optimization Conference*, 2011, pp. 297-300, doi: 10.1109/PEOCO.2011.5970452.

[14]S. Song, J. Liu, S. Ouyang, X. Chen and B. Liu, "Control of Direct AC/AC Modular Multilevel Converter in Railway Power Supply System," *2018 International Power* Electronics *Conference (IPEC-Niigata 2018 -ECCE Asia)*, Niigata, Japan, 2018, pp. 1051-1055, doi: 10.23919/IPEC.2018.8508001.

[15]Y. N. Vijaykumar, V. Vemulapati, N. Visali and K. Raju, "Railway Power Supply System using Modular Multilevel Converter with Droop Characteristics," *2020 4th International Conference on Electronics, Communication and Aerospace Technology (ICECA)*, Coimbatore, India, 2020, pp. 12-20, doi: 10.1109/ICECA49313.2020.9297599.

[16]L. Min and X. Mou, "Simulation Analysis of Railway Co-phase Power Supply System based on Inequilateral Scott Connection Transformer," *2018 5th IEEE International Conference on Cloud Computing and Intelligence Systems (CCIS)*, Nanjing, China, 2018, pp. 1066-1071, doi: 10.1109/CCIS.2018.8691143.

[17]Y. Hu et al., "A Partial-Capacity Converter for Advanced Co-phase Traction Power Supply System," *2019 IEEE Energy Conversion Congress and Exposition (ECCE)*, Baltimore, MD, USA, 2019, pp. 6333-6337, doi: 10.1109/ECCE.2019.8912919.

[18]Infineon, "FZ1800R45HL4: 4500 V, 1800 a single switch IGBT module - Infineon technologies" https://www.infineon.com/cms/en/product/power/igbt/igbt-modules/fz1800r45hl4/ (accessed Jun. 29, 2023).

[19]R. Teodorescu, M. Liserre, and P. Rodríguez, "Grid Converters Control for WTS," in Grid converters for photovoltaic and Wind Power Systems, Hoboken: Wiley-IEEE Press, 2023

[20]Z. Weifeng, C. Yanbo, G. Leijiao and T. Wen, "Study on double modulation wave carrier-based PWM for three-level neutral-point-clamped inverters," *2013 5th International Conference on Power Electronics Systems and Applications (PESA)*, Hong Kong, China, 2013, pp. 1-5, doi: 10.1109/PESA.2013.6828204.

[21]S. Debnath, J. Qin, B. Bahrani, M. Saeedifard and P. Barbosa, "Operation, Control, and Applications of the Modular Multilevel Converter: A Review," in *IEEE Transactions on Power Electronics*, vol. 30, no. 1, pp. 37-53, Jan. 2015, doi: 10.1109/TPEL.2014.2309937.

[22]G. Wenming and M. Longhua, "Control principles of micro-source inverters used in microgrid," *Protection and control of modern power systems (2016),* 1:5 doi: 10.1186/s41601-016-0019-8

[23]J. Rocabert, A. Luna, F. Blaabjerg and P. Rodríguez, "Control of Power Converters in AC Microgrids," in *IEEE Transactions on Power Electronics*, vol. 27, no. 11, pp. 4734-4749, Nov. 2012, doi: 10.1109/TPEL.2012.2199334

[24]A. Shahariari, H. Mokhlies, A. H. Bin Abu Bakar and M. Karimi, "The numerical estimation method of series FACTS compensator based on injection model of voltage source inverter," *2011 IEEE Symposium on Industrial Electronics and Applications*, Langkawi, Malaysia, 2011, pp. 490-494, doi: 10.1109/ISIEA.2011.6108760.